From boulders to planetary systems

Hubert Klahr

Max-Planck-Institut für Astronomie, Königstuhl 17, 69117 Heidelberg, Germany

Abstract

In this chapter we will give a brief overview on our current theoretical understanding how planets form from the solid material in circumstellar disks in the *core accretion-gas capture* model. This chapter will not be as concise and complete as a review on this matter, yet will serve as an introductory text to generate interest in the subject. Students are referred to comprehensive text books and some important reviews.

This chapter will discuss "dusty storms", e.g. the dust transport in turbulent protoplanetary disks, followed by the latest model of planetesimal formation, e.g. gravoturbulent planetesimal formation, which deals with particle concentration in turbulence and N-body simulations thereof. We also briefly describe the core accretion - gas capture process and talk about nascent planets, e.g. the observability of planet-disk interaction concluding with the migration of young planets and the final arrangement of planetary systems.

Key words: accretion, accretion discs, stars: pre-main-sequence, planetary systems: protoplanetary discs, planetary systems: formation

1 Introduction

Planet formation is most likely not one single process, as it is likely in the case of star formation, but consists of several consecutive steps each building upon the material produced in the previous steps. The first step is the growth of dust in circumstellar disks to larger and larger aggregates via collisional sticking. This process is extensively discussed in the chapter by Alexander. Sticking ends with centimeter to meter-sized objects; just imagine throwing sand and stones together while sitting at the beach: macroscopic objects do not stick. Thus we need a new mode of growth to continue to planets.

Email address: klahr@mpia.de (Hubert Klahr).

The next hypothesized milestones in planet formation are the kilometer-sized planetesimals. They are the first objects to be bound by gravity. Thus it was already early on speculated that they should form via a gravitational collaps of the dust content of the disk (see Fig. 1). We will learn in this chapter that this process is still not completely understood even there were some recent major break throughs.

Once there are planetesimals they start interacting via gravity and form larger and larger objects in successive collisions. In this manner the precursors of the terrestrial planets come to life and the cores of the gas giants. Most planetesimals were incorporated into the planets, yet one can regard the asteroids and the comets as the last witnesses of the former planetesimal population.

When the cores of the future giant planets are massive enough they start accreting gas via gravity. They also interact over large distances gravitationally with the gas of the disk, with the abundant planetesimals and also with the other planets. All of these interactions lead to exchange of angular momentum and thus to changes in the orbital parameters of the planets: mainly the semi major axis, but also eccentricity and inclination. Finally the planets will assume a more or less stable orbit, a precondition for a stable climate over billions of years, which is a precondition to develop life as in the case of our earth.

There is an alternative theory of planet formation, which describes planet formation as being star formation on a smaller scale. Just like stars condensate out of the gas phase it is hypothesized that a gravitational instability could lead to the fragmentation of clumps in the circumstellar disk. This theory has notably problems to explain terrestrial planets and the massive cores of giant planets yet we include a brief description of the theory for the sake of completeness. Please see also the discussion of this model in the chapter by Lodato.

1.1 Disk Instability Model

Boss (1997, 2001) proposed a model in which a cool protoplanetary disk, with roughly 10% of the mass of the star, fragments as a consequence of its self gravity and spontaneously forms multiple giant planets within a few orbital periods. The fundamental problem with this model is that it needs an almost isothermal gas to allow for the collapse and to keep the Toomre parameter low. Gammie (2001) shows that the cooling time $t_{\rm cool}$ has to be smaller than an orbital period $t_{\rm orb}$.

$$t_{\rm cool} < \frac{3}{\Omega} \approx \frac{1}{2} t_{\rm orb}. \qquad (1)$$

Radiative diffusion within a dust-rich disk as well as in a self-gravitating blob is too inefficient to allow for such high cooling rates. Also the recently invoked thermal convection can only slightly increase the efficiency of the cooling; they show that the maximum fraction of the energy carried vertically outward through a disk by convection is about 20%. Convection in itself does not result in energy loss from the disk; it only transports the heat to the surface where it still has to be radiated away. Even if strong convection would be able to transport energy in the interior of the disk (Boss 2004) the gas would still have to radiate at the surface as a black body, at a maximum rate proportional to T^4, where T is the central temperature in the disk. The cooling time would then be longer than an orbital period for radii out to 33 AU:

$$t_{\rm cool} \approx \frac{\Sigma c_v}{2\sigma} T^{-3} = \frac{\Sigma}{10^3 \text{ g cm}^{-2}} \left(\frac{T}{50\text{K}}\right)^{-3} \times 190 \text{ yrs.} \quad (2)$$

Here we used typical surface densities Σ and temperatures T from the Boss model (Boss 2001); c_v is the specific heat and σ is the Stefan-Boltzmann constant. Note that for even only slightly smaller temperatures the cooling time increases dramatically. We argue on the basis of this estimate that it is possible to form brown dwarf companions out of an extended circumstellar disk at large radii but not planets at the distances of Jupiter or Saturn (see also Rafikov 2005, 2007). Basically one can conclude that the conditions needed for planet formation by gravitational instability are unlikely to occur in protoplanetetary disks.

The following sections will discuss the single steps in the core accretion - gas capture model in a bit more detail, yet for a complete picture of planet formation we refer to the review by Jack Lissauer (Lissauer, 1993) and the book "Planet Formation - Theory, Observations, and Experiments"(Klahr and Brandner, 2006).

2 Shearing Box Simulations of Turbulent Diffusion in Protoplanetary accretion disks

Circumstellar disks are assumed to be turbulent (see also the chapter by Lodato and by Ferreira) as this is the only way to explain the observed accretion rate in such systems (see Fig. 2). If disks are young, they are assumed to be massive and cold. In this situation self gravity leads to angular momentum transport and turbulence (see Lodatos chapter). As the mass of the disk eventually decreases, the disk will be too warm and too light for self-gravity. Now magnetic effects can take over by braking the disk with a background field, or by generating turbulence (see chapter by Ferreira).

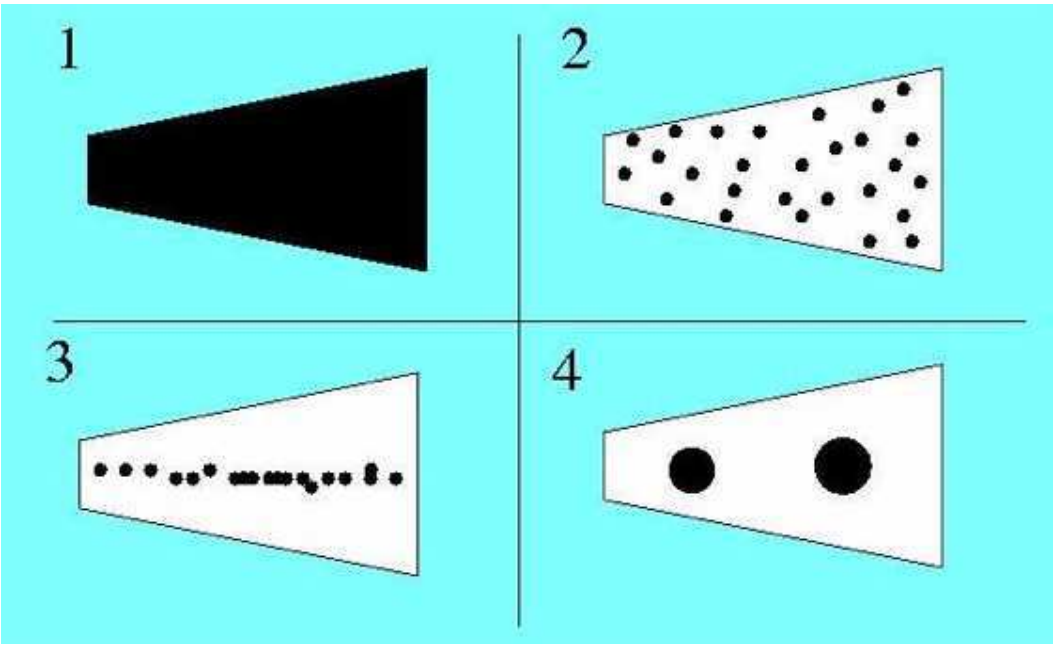

Fig. 1. Dust coagulates to larger grains, eventually sediments to the midplane of the disk and forms larger gravitationally bound objects, e.g. planetesimals.

The turbulence is a prerequisite to transport (diffuse) angular momentum radial outward in not-self-gravitating disks. The local lack in angular momentum then leads to the accretion of matter towards the star (see Fig. 3).

The magnetorotational instability (Balbus and Hawley, 1998) is known to drive strong turbulence in accretion disks and can easily be explored in numerical simulations. One should notice that this instability needs a certain minimum ionization of the disk either provided by thermal ionization where temperatures are sufficient or elsewhere by energetic radiation penetrating the disk. This radiation can originate from background sources and from the central object, e.g. X-rays alike.

Dust grains are a natural enemy of ionized gas as the free electrons get easily trapped on the dust grain surfaces. It is not sufficient to have ions and charged dust grains for the magnetorotational instability, as both have a low charge per mass ratio and there is only weak coupling to the magnetic fields. One really needs free electrons in an abundance to allow for a magnetic Reynolds number of about 100 to drive turbulence (Balbus and Terquem, 2001).

As a result it is currently an open question which parts of the disk may be turbulent by the magnetorotational instability. It is widely accepted that there is a zone deeply embedded in the disk (Dead Zone; see Fig. 4) which is too cold and dusty for magnetic effects, yet it is under debate where this zone is located and what its dynamical behavior is. The chapter by Ferrera deals with the details of dead and active zones.

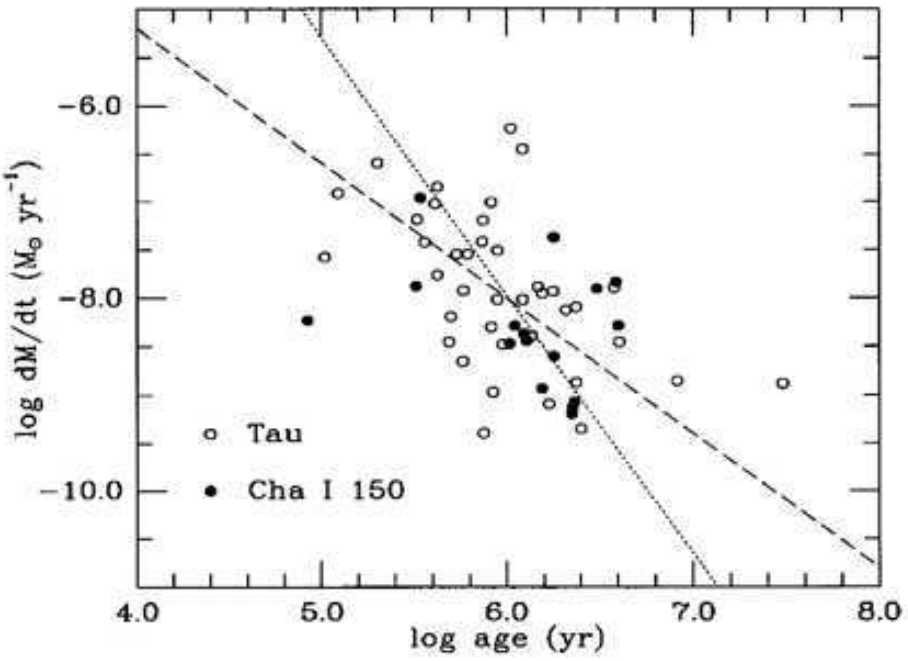

Fig. 2. Mass accretion rate vs. age. Stars in Taurus (open circles) and in Chamaeleon I (filled circles), the last at a distance of 150 pc. Dashed lines, least-square best fit assuming that the error in log t is 0.3, while the error in log dM/dt is 0.6. Dotted lines, least-square best-fit assuming that the error in both log t and log dM/dt are 0.4. The dashed line fits are preferred because the errors in estimating accretion rates, along with the intrinsic dispersion of accretion at a given age, are likely to be larger than the differential errors in stellar ages. With kind permission reprinted from Hartmann etal. 1998

Nevertheless in the following we will ignore this effect for the sake of simplicity. The potential influence of the Dead Zone on the planet formation process is still widely speculative, yet interesting results can be expected in the near future.

3 Particle motion

Particles tend to move differently with respect to gas for one obvious reason: they do feel most of the forces the gas does, e.g. gravity, Coriolis and centrifugal accelerations, but neither thermal nor magnetic pressure. On the other hand they feel friction from the gas if they move with a different velocity (e.g.

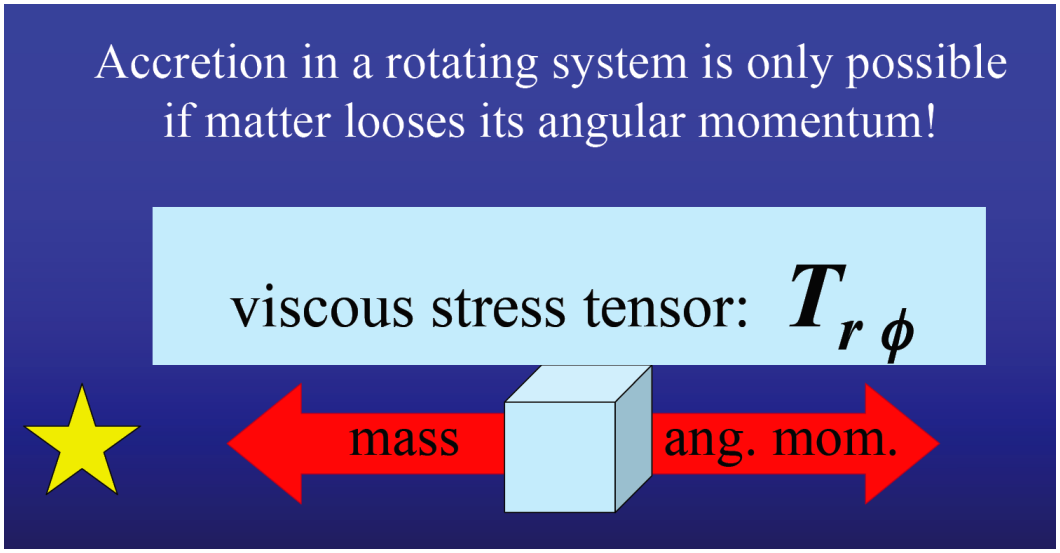

Fig. 3. The observed accretion can only occur if there is angular momentum transport in the disk. A widely accepted explanation for this angular momentum transport is turbulence, see review by Lodato.

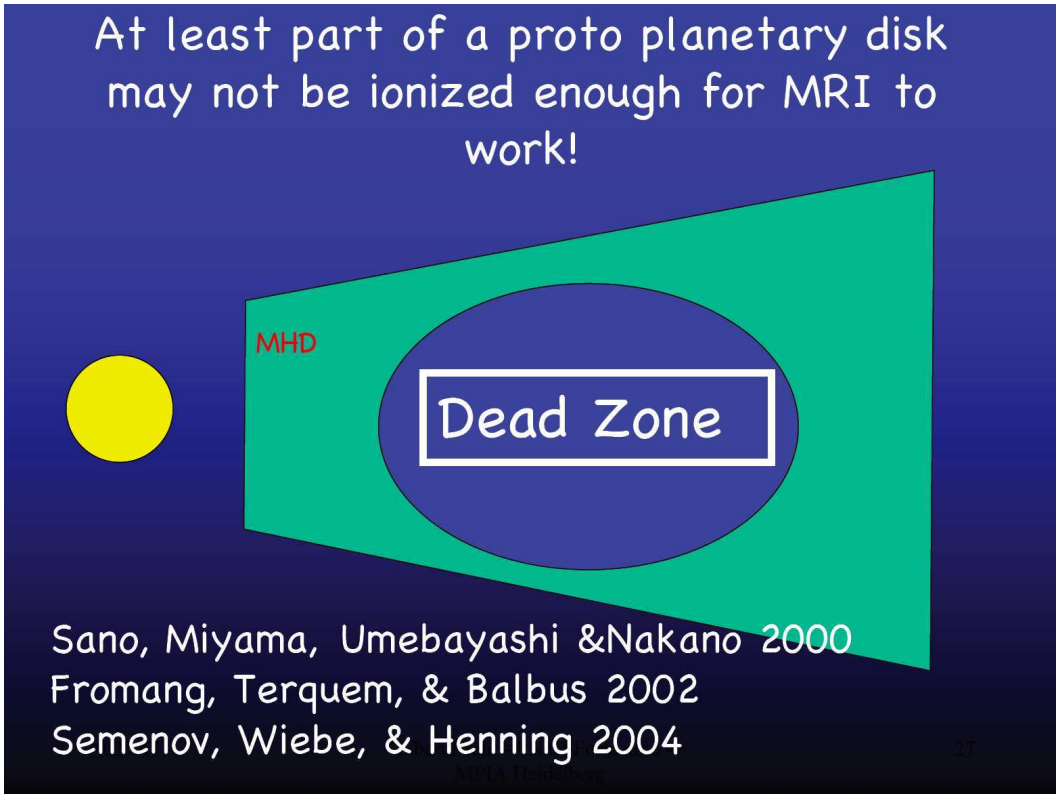

Fig. 4. The existence of turbulence depends depends on the presence of instabilities. The magnetorotational instability for instance requires a certain ionization rate. Wherever this ionization is too low due to high column density and low temperature one expects a non-turbulent zone, popularized as Dead Zone.

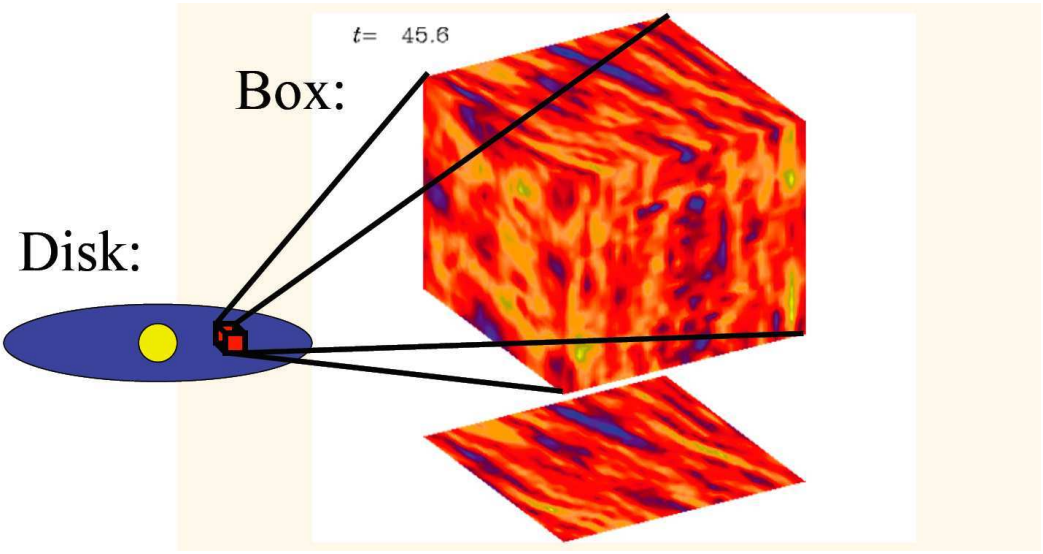

Fig. 5. For turbulence simulations in accretion disks one often works in shearing box coordinates. This means instead of treating a global disk, one focuses on a small Cartesian box cut out of the disk. The benefit of this local approach is better resolution and a minimization of boundary effects. However, this approach has also a few limitations (as discussed by, for example, King et al. 2007) - in particular that shearing box calculations always result in an alpha value that is an order of magnitude smaller than observed in real systems.

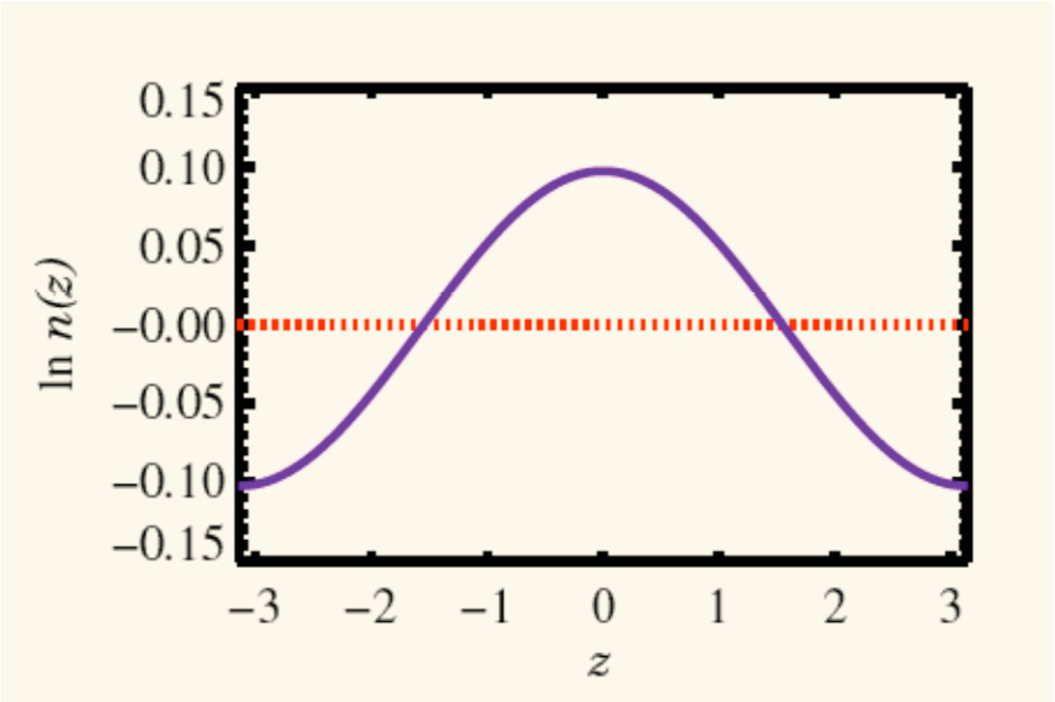

Fig. 6. Gravity makes dust sediment, yet turbulence lifts it up again. This turbulent diffusion can then be measured by the scale-height in the dust layer.

Run	$\alpha_t/10^{-3}$	$\alpha_t^{(mag)}/10^{-3}$	$D_z^{(t)}/10^{-3}$	$D_x^{(t)}/10^{-3}$	Sc_z	Sc_x
64a_z,x	0.33 ± 0.08	1.47 ± 0.29	1.16 ± 0.12	2.07 ± 0.26	1.55	0.87
64b_z,x	0.33 ± 0.08	1.47 ± 0.29	1.16 ± 0.12	2.07 ± 0.26	1.55	0.87
64c_z,x	0.33 ± 0.08	1.47 ± 0.29	1.12 ± 0.14	2.12 ± 0.75	1.61	0.85
128a_z,x	0.18 ± 0.04	0.83 ± 0.18	0.77 ± 0.12	1.24 ± 0.17	1.31	0.81
128c_z,x	0.18 ± 0.04	0.83 ± 0.18	0.79 ± 0.13	1.27 ± 0.30	1.28	0.80

Fig. 7. The first column gives the name of the run and the resolution, the second and third the strength of the turbulent stresses in its non-magnetic (Reynolds) and magnetic (Maxwell) stresses. The fourth and fifth column gives the vertical and radial diffusivity, whereas the last two columns give the resulting vertical and radial Schmidt numbers. Reprinted from Johansen and Klahr 2006.

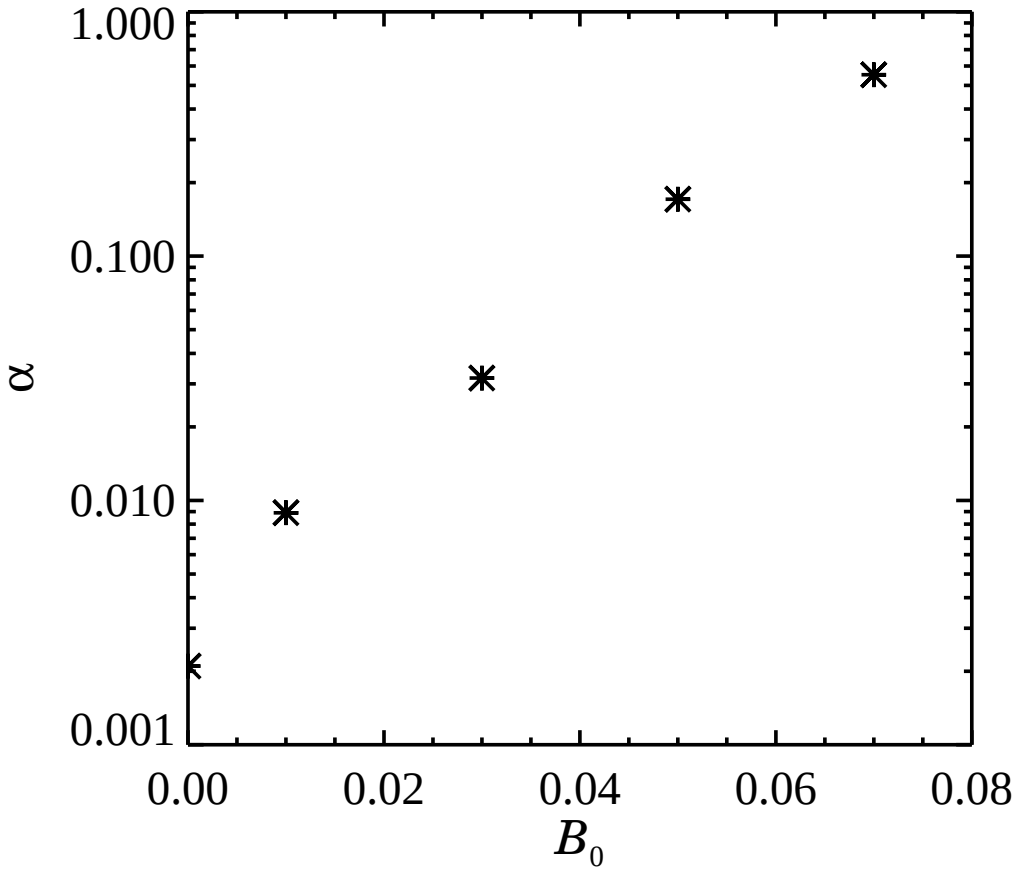

Fig. 8. The α value (strength of turbulence) as a function of the strength of the imposed vertical field. A stronger background field leads to stronger turbulence. Reprinted from Johansen et al. 2006.

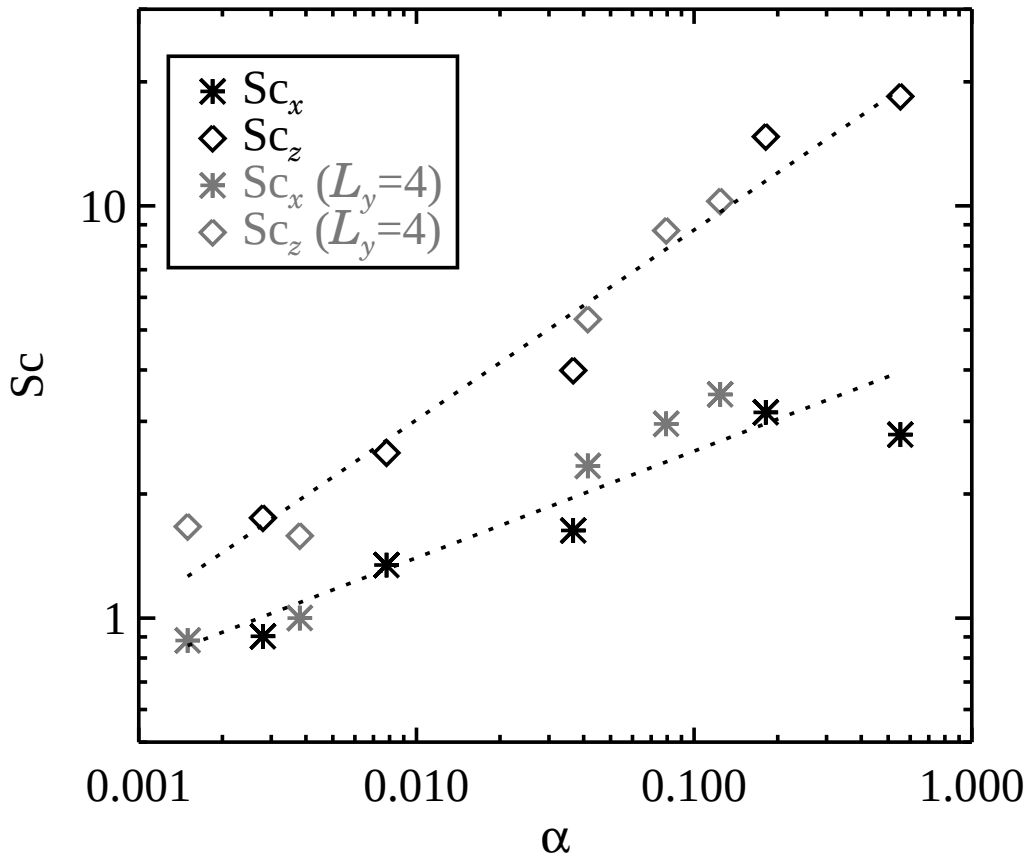

Fig. 9. The Schmidt number plotted against the α value and the best power-law fit (dotted lines). The best fit has $\mathrm{Sc}_x = 4.6\alpha^{0.26}$ and $\mathrm{Sc}_z = 25.3\alpha^{0.46}$. Reprinted from Johansen et al. 2006.

velocity vector $\vec{v_d}$) than the gas (e.g. $\vec{v_g}$) which is given via:

$$\vec{f}_{friction} = -\frac{\vec{v_d} - \vec{v_g}}{\tau_f}. \tag{3}$$

Small particles couple quickly to the surrounding gas motion, e.g. they have a short coupling (or stopping) time τ_f and as a result the frictional term is strong. Larger particles take longer to lose their momentum with respect to the gas (longer τ_f), because their frictional acceleration is smaller. Based on this concept one estimates the terminal velocity a particle will approach as a function of its friction time τ_f. One can easily understand that particles closely coupled to the gas move up any pressure gradient: Any particle motion v_d with respect to the gas velocity v_g can only occur if there is a mismatch in the forces acting on the two components. For small particles most forces are identical to the forces acting on gas, e.g. gravity, centrifugal and Coriolis forces. The only difference is in the pressure p (thermal and magnetic) which is only felt by the gas. Subtracting the equations of motion for dust and gas

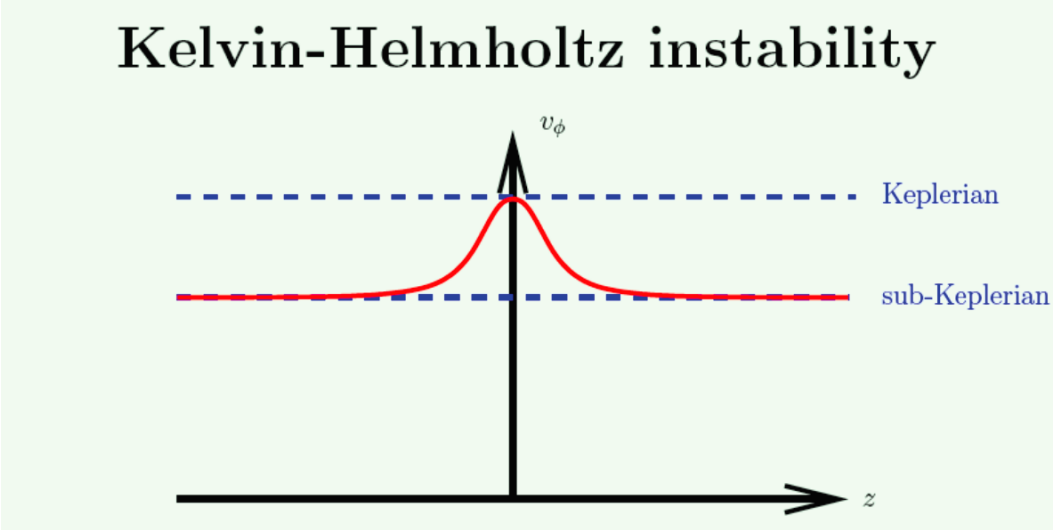

Fig. 10. The general radial pressure gradient lets the disk rotate slower than the Keplerian value. Yet when dust sediments to the midplane and concentrates there to higher densities than the gas density, then the dust starts dominating the dynamics and forces the gas on a Keplerian value. As a result there is shear induced in the vertical direction. This shear becomes unstable to the Kelvin Helmholtz instability, which starts stirring up the dust eventually preventing gravitational collapse of the dust sub-layer.

under the influence of forces

$$\partial_t \vec{v_g} = -\frac{1}{\rho}\vec{\nabla} p + \vec{forces} \tag{4}$$

$$\partial_t \vec{v_d} = -\frac{\vec{v_d} - \vec{v_g}}{\tau_f} + \vec{forces}, \tag{5}$$

and assuming the velocities to change slower than the coupling time τ_f one can get to the simple equation

$$\vec{v_d} = \vec{v_g} + \tau_f \frac{1}{\rho}\vec{\nabla} p. \tag{6}$$

As a result the dust moves up any pressure gradient, be it the global gradient towards the central star or the midplane of the disk. Local pressure fluctuations like vortices and pressure bumps can concentrate dust via this mechanism.

4 Diffusion

The turbulence in the active zones not only diffuses angular momentum but also dust grains and molecules. This diffusion can be measured in local simula-

tions of magnetorotational turbulence (see Fig. 5 and 6). For this measurement one can you as an artificial force field acting on the particles, which will try to concentrate particles locally. Diffusion tries now to move particles away from the concentration and eventually an equililibrium between forced drift or sedimentation is reached with the diffusion. If one uses for instance an artificial sinusoidal force field

$$g_z = -g_0 sin(k_z z), \tag{7}$$

it will concentrate the dust around the $z = 0$ midplane. Putting this term in the equation for vertical particle transport together with the diffusion term one can derive a condition when the sedimenting flux and the diffusion flux j_d cancel each other. The sedimentation flux is given by:

$$j_s = v_z n_{dust} = -g_0 sin(k_z z)\tau_f n_{dust}, \tag{8}$$

with n_{dust} being the dust number density and τ_f the coupling time between dust and gas, e.g. the time a force free particle would need to stop with respect to the gas. And the diffusion flux j_d is given by:

$$j_D = -D_z \nabla n_{dust}, \tag{9}$$

Both fluxes shall cancel each other.

$$-g_0 sin(k_z z)\tau_f n_{dust} = -D_z \nabla n_{dust}. \tag{10}$$

The analytic solution is now simply:

$$\ln n(z) = \ln n(0) + \frac{\tau_f g_0}{k_z D_z} \cos(k_z z), \tag{11}$$

which is a cosine in the logarithmic particle density. The amplitude of this cosine can now directly translated in the diffusivity D of the system.

It is interesting to notice that this diffusion is "an-isotropic", e.g. radial diffusion (with diffusivity D_r) is stronger than the vertical diffusion (with diffusivity D_z) , which can be expressed as Schmidt numbers S_c.

$$S_{cr} = \frac{\nu}{D_r} \quad S_{cz} = \frac{\nu}{D_z} \tag{12}$$

Schmidt numbers are the ratio between viscosity (ν) and diffusivity (see Fig. 7).

Besides the ionization degree it is the ambient background magnetic field that determines the strength of the turbulence (see Fig. 8). While this is true in simulations, it should be noted that the existence of such background fields is far from certain in real discs, and that it is not clear which of the (imposed) field geometries used in simulations is in fact the most relevant to real systems (e.g., King et al. 2007). Both viscosity and diffusivity increase with the strength of a magnetic field threading the disk (Hawley et al. 1995), yet diffusivity responds weaker to the stronger turbulence than does viscosity (Johansen, Klahr and Mee 2006). As a result the Schmidt number decreases with an increase of the turbulence strength (see Fig. 9). It is now very unfortunate that we have no measurements of the magnetic field threading protoplanetary disks.

It should be noted that also in the case of no ionization, and thus not magnetohydrodynamic instability, there will be some turbulence in the disk. If the dust sediments towards the midplane in a laminar (e.g. non-turbulent) disk it generates vertical shear and Kelvin Helmholtz turbulence (see Fig. 10 and 11).

This phenomenon can also be observed in the earth atmosphere whenever there is vertical shear in the wind speed. The Kelvin Helmholtz modes show as periodic "ripples" in the cloud pattern. [1] This kind of turbulence is too weak to explain the observed accretion rates, yet is strong enough to prevent sedimentation of dust and thus the occurrence of the Goldreich-Ward instability (see below).

If one is studying the diffusion properties of magnetohydrodynamical turbulence (Johansen and Klahr, 2005) (see Fig. 6) one can notice certain fluctuations in the local dust to gas ratio. In particular we simulated sedimentation of small grains up to 1cm in size in the effective gravitational potential of the disk-star system [2] (see also Fig. 21). The measured fluctuations in the relative density were on the order of 20% for centimeter-sized objects but a lot smaller for submicron sized dust. These density fluctuations result from the turbulence as well. In the following we will discuss a few different mechanisms to trap and segregate particles.

[1] Check out: http://en.wikipedia.org/wiki/KelvinHelmholtz_instability for nice images.

[2] Unhindered sedimentation would lead to very high particle densities in the midplane, e.g. a dust layer so thin that the mechanism proposed by Goldreich and Ward (1973) would lead to gravitational fragmentation and planetesimal formation. Nevertheless, turbulent diffusion transports material away from the midplane, explaining why self-gravity of the dust component and gas turbulence in the disk seem to be mutually exclusive.

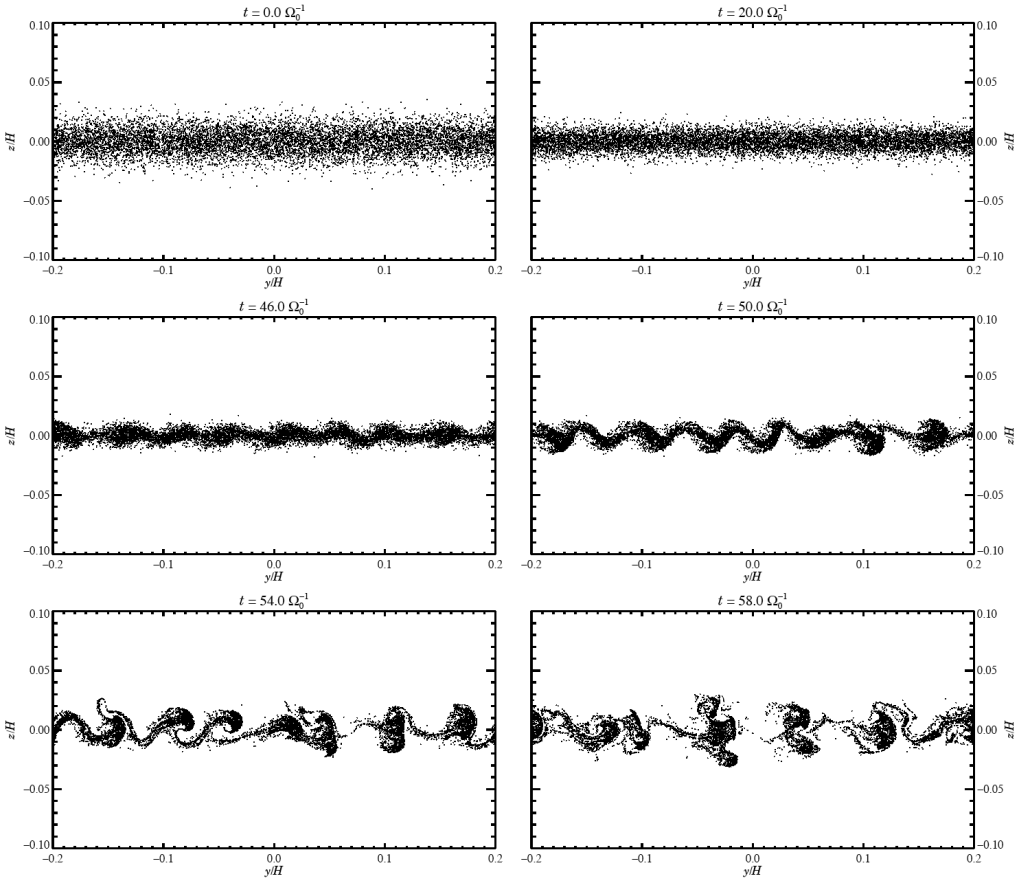

Fig. 11. The onset of the Kelvin-Helmholtz instability for cm-sized pebbles with $\Omega_0 \tau_\mathrm{f} = 0.02$. The initial Gaussian particle distribution falls towards the mid-plane of the disk on the characteristic time-scale of $t_\mathrm{grav} = 1/(\Omega_0^2 \tau_\mathrm{f}) \approx 50 \Omega_0^{-1}$. The increased vertical shear in the gas rotation velocity eventually makes the disk unstable to the KHI, forming waves that finally break as the turbulence goes into its non-linear state.

The disk temperature and density decrease with the distance from the central object and thus there is a global pressure gradient in the disk pointing radially outward. This radial pressure gradient supports the disk against gravity from the central object and the centrifugal force is reduced to a sub-Keplerian rotation rate by a few permille.

Even this small sub-Keplerian rotation can lead to a dramatic "rain out" of a certain size particles radially into the central star because they will move up the pressure gradient. The critical size is reached when the particle growth time via sweeping up smaller dust grains becomes larger than the radial drift time (See Fig. 12).

In the case of no external forces the effect of turbulent concentration would be simple: Centrifugal forces would expel particles from turbulent eddies and concentrate them in convergence zones between the vortices (See Fig. 13). In

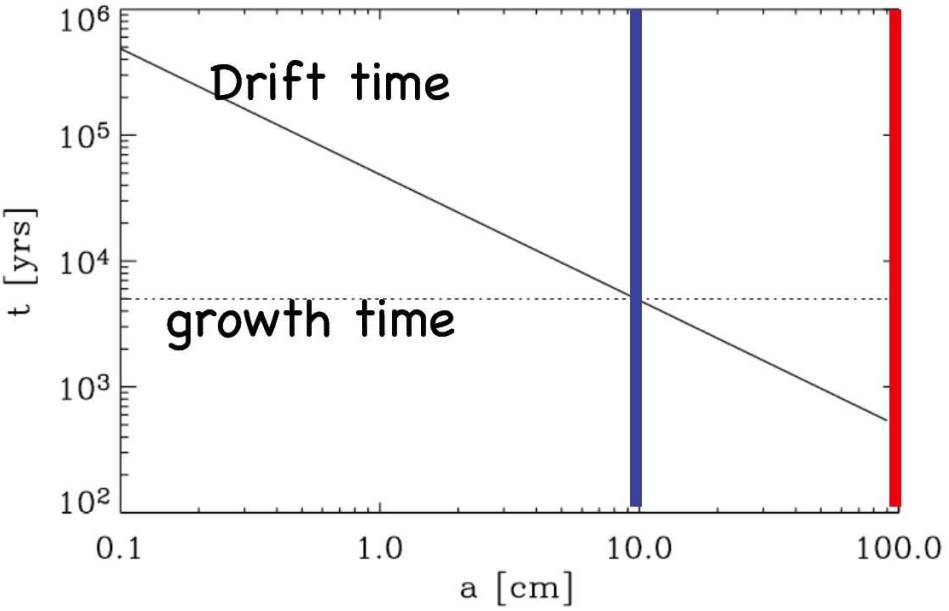

Fig. 12. Comparison between drift time (solid line) and growth time (dotted line) for solids as a function of size. The values are calculated using the equations from this paper for a location of 7.5 AU in a minimum mass solar nebula. Taken from Klahr and Bodenheimer 2006

the accretion disk this can only be the case on the very shortest length scales of turbulence, e.g. a few hundred to a few thousand meters. All the larger scales are rotating so slow, that the motions get influenced by the global rotation of the disk.

Just as in the case of earth turbulence there is a strong influence of the Coriolis forces for a large flow structure as in the case of high and low pressure regions determining our weather pattern on earth, yet there is negligible influence on fast and small scales, like the turbulence in our bath tub. The myth about water running out of the bath tub forming a left rotating eddy on the Northern hemisphere and a right rotating eddy on the southern is thus a pure legend as can be shown by simple estimates on the strength of the Coriolis forces on those scales. One actually needs high precision measurements under lab conditions to see the effect, conditions which are never fulfilled in our kitchen sink experiment.

The vertical gravity gradient in the disk is another source of trapping particles in turbulence. This was the first time discovered for thermal convection in disks but should apply in any 3D turbulent pattern of an accretion disk as long as the vortex frequency is lower than the local Keplerian frequency (see Fig. 14). Also here particles try to sediment to the mid-plane, the location of highest pressure. Yet the gravity decreases with getting closer to the mid-plane, in fact for small z(e.g. z smaller than a few pressure scale heights) the

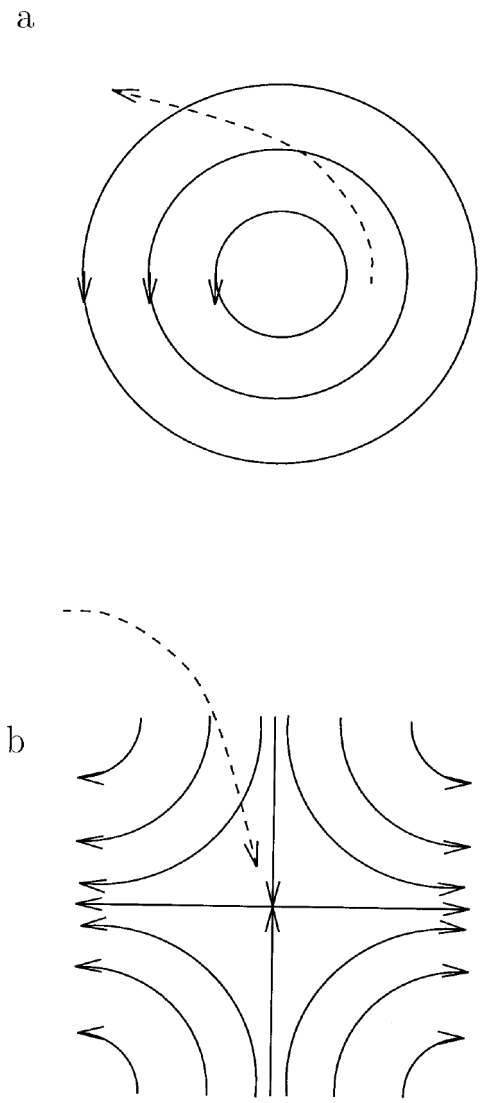

Fig. 13. Under laboratory-observed conditions particles (a) spiral out of the vortices (eddy), but (b) collect in convergence zones (strain fields). Taken from Klahr and Henning 1997.

vertical gravitational acceleration g_z can be written as a function of the orbital frequency of the disk Ω and the height above the midplane z:

$$g_z = -\Omega^2 z. \tag{13}$$

This is an harmonic oscillator. If there is now a vertical turbulent vortex, then dust gets trapped in it due to the combination of rotation and differential settling (see Fig. 15).

A much simpler mechanism to trap particles and stop them drifting into the central object is a radial pressure bump as it may occur in disks as laminar

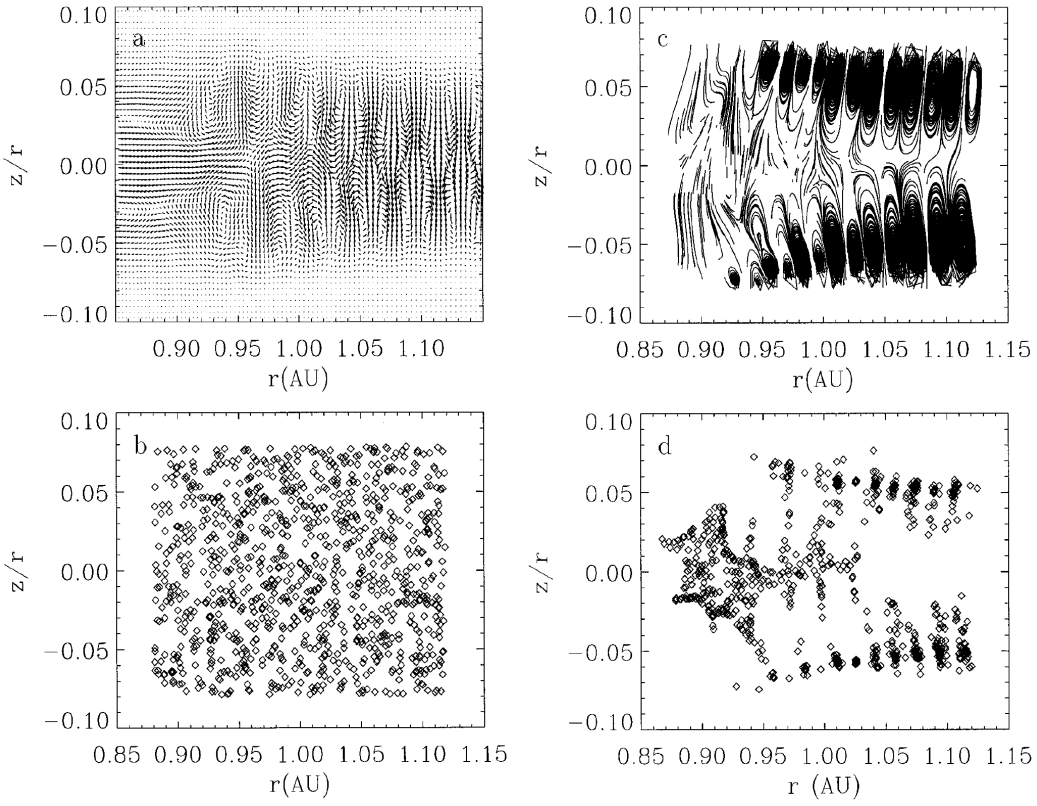

Fig. 14. (a) Mass flux in the convective region of a protoplanetary accretion disk. This is the result of a 2D radiation hydrodynamical simulation. (b) The homogeneous initial distribution of 0.1-cm grains. (c) The traces of a part of the grains during 160 years. (d) The position of the grains after 160 years. Taken from Klahr and Henning 1997.

features or as turbulent fluctuations (see Fig. 16).

Vortices in the mid-plane of the disk are another source of particle segregation (Barge and Sommeria, 1995). These again can either be long-lived vortices like the weather pattern on earth, e.g. the anti-cyclonic high pressure regions or short-lived fluctuation in the velocity pattern of the turbulence. Yet the effect was first pointed out for long lived anti-cyclonic vortices, where Coriolis forces concentrate large particles and the pressure maximum concentrates smaller dust (see Fig. 17).

Coming back to the first 3D simulations of particle trapping in magnetohydrodynamical turbulence (Johansen and Klahr, 2005) (see Fig. 6) we identified the vortex trapping mechanism ala Barge and Sommeria and pressure maxima trapping as the important effects (see Fig. 18). In order to understand the coupling mechanism and the physical effect that drives the fluctuations we plotted the density fluctuations as a function of the local vorticity and found a strong anti-correlation (see 18). This behavior, e.g. concentration of dust in anti-cyclonic vortices, was already discovered by Barge and Sommeria (1995)

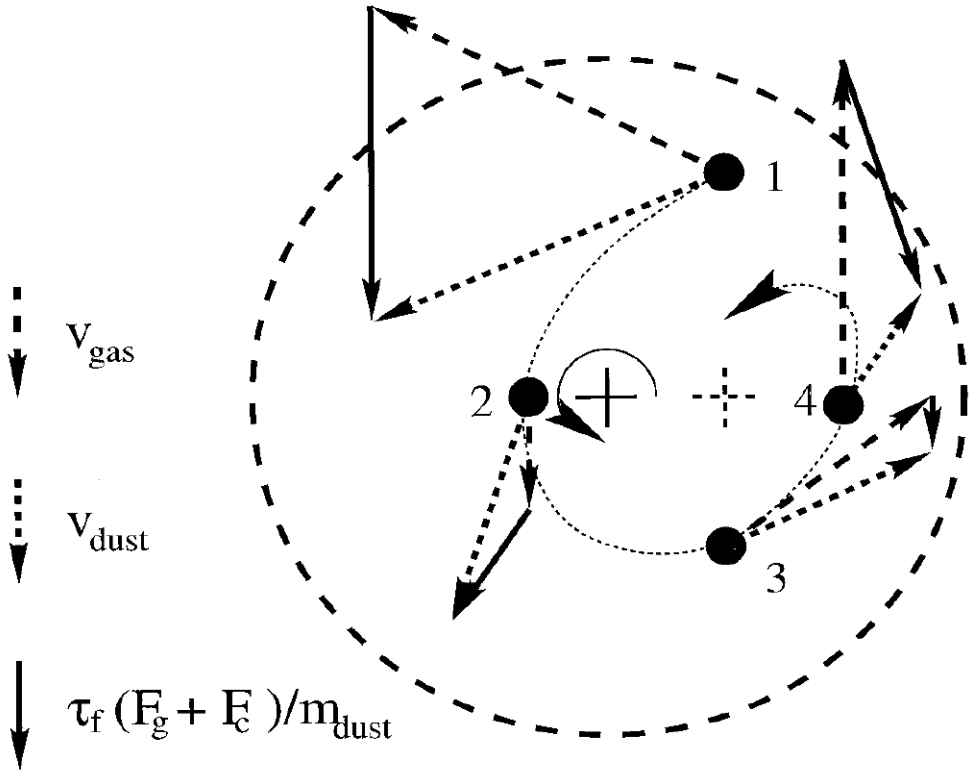

Fig. 15. The mechanism of particle concentration can be understood by considering the acting forces. Four particle positions are displayed. The dashed arrows indicate the local gas velocity. The solid arrows stand for the gas-particle relative velocities which are induced by the sum of gravitational and centrifugal forces (i.e., the acceleration $(F_g + F_c)/m_{dust}$ The capability of the eddy for collecting particles depends times the friction time). Thus, the solid arrows indicate the actual particle movement. On location 1, where the particle has the largest height above the midplane, the gravitation dominates over the centrifugal force and the particle lifting gas drag. Here, the particle moves closer toward the equilibrium point (indicated by a dashed cross). At point 2 as well as at point 4, the centrifugal force causes the particle to drift away from this equilibrium point, while gravitation and gas drag point in a tangential direction, not contributing to a radial motion. Finally location number 3 is the closest to the midplane and the gravitational force the smallest. At points 1 and 3 the particle is spiraling inward, while at points 2 and 4 it is spiraling outward. As long as the centrifugal effects are smaller than the effects caused by the gradient in the gravitational acceleration, the particle undergoes a net motion toward its equilibrium point. Taken from Klahr and Henning 1997

for static large scale vortices. We now found that this effect is also dominant if the vortices are of limited life time as they are generally generated and destroyed in turbulence as it is in the case for the magnetorotational instability studied here.

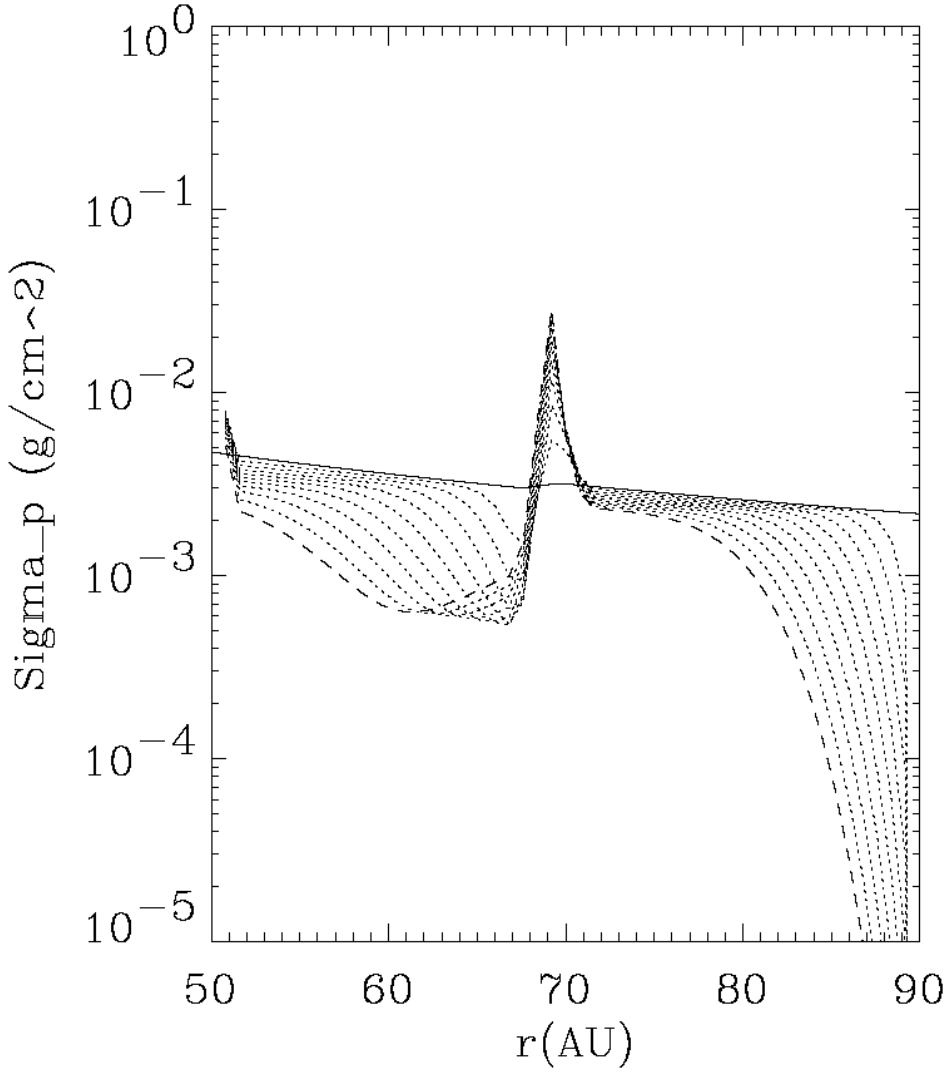

Fig. 16. Dust capture at a small radial pressure maximum. Evolution of the 600 μm size particle surface density distribution for a model of a gas poor circumstellar disk. The solid line gives the initial distribution. The following lines are snapshots every 400 yr. Reprinted from Klahr and Lin 2000.

If the particle concentration occurs in a long lived vortex, huge amounts of solid material can be accumulated which would certainly boost any kind of planet formation process (Klahr and Bodenheimer, 2006). On the other hand if the vortices are only short-lived fluctuations of the general turbulence pattern, then there is also a measurable effect in the fluctuations of the particle denisity (see Fig. 19). As now the particles get trapped once in a while in a vortex they can not drift unhindered into the central object, which shows as a significant reduction of the mean drift rate (see Fig. 20).

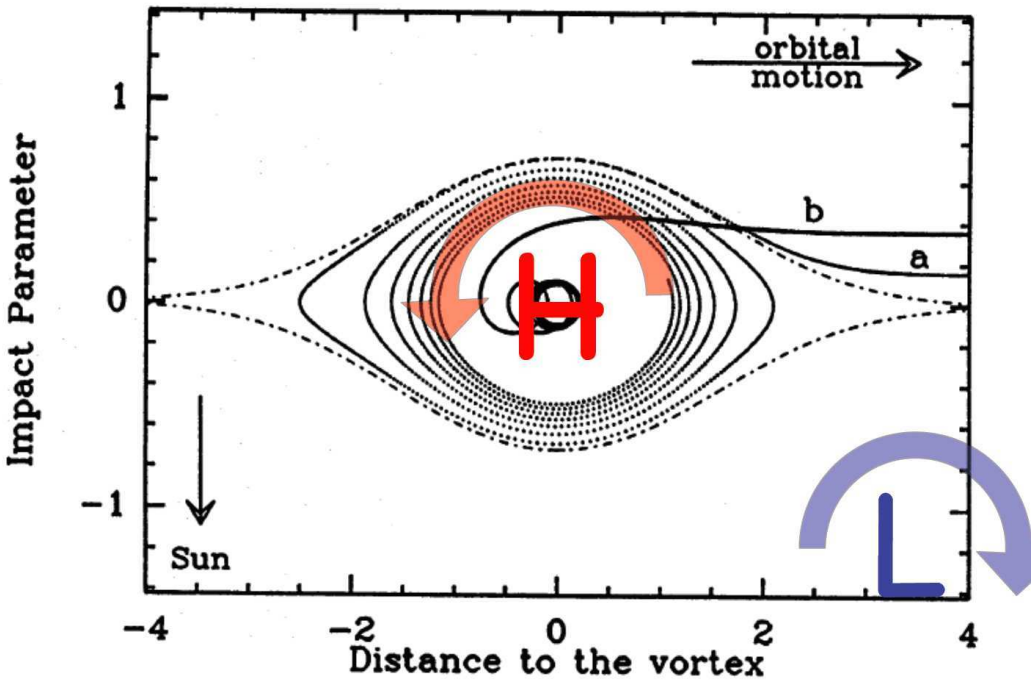

Fig. 17. Trajectories of the particles in a gaseous vortex sketched by the separatrix (dashed line) between open and closed streamlines. The particles penetrate into the vortex and spiral inward toward its center; they tend to reach purely epicyclical motion with a transient behavior strongly dependent on the friction parameter: light particles ($\tau_f\Omega = 0.05$ in case (a)) remain near the edge of the vortex, whereas heavy ones ($\tau_f\Omega = 3.0$ in case (b)) first sink deeply into the inner regions. It must be noted that, for clarity of the figure, the coordinates have been expanded by a factor of two. With kind permission reprinted from Barge and Sommeria 1995. The center of an anticyclonic vortex is also a pressure maximum explaining the particle trapping in an alternative way.

5 Planetesimals and the "meter-barrier"

Planetesimals are several-kilometer-sized objects in the solar nebula, which are believed to be the building bricks for planets. Whereas there is no observational evidence for their existence in circumstellar disks, it is generally accepted that asteroids and comets are the last survivors from this class of objects. The behavior of planetesimals is quite distinct from the behavior of smaller, e.g. meter-sized objects. The meter-sized boulders feel a head wind as they need to move on a Keplerian orbit to balance the stellar gravity by centrifugal acceleration, whereas the disk is supported by its radial pressure gradient and rotates at a sub-Keplerian rate. As a result the boulders drift radially inwards towards the star. In general any solids will always move up the local pressure gradient. The drift rates can be dramatic, as for meter-sized objects the typical drift time becomes smaller than the growth time due to sweep up of smaller dust and debris (see Fig. 12). This way they get lost into the star

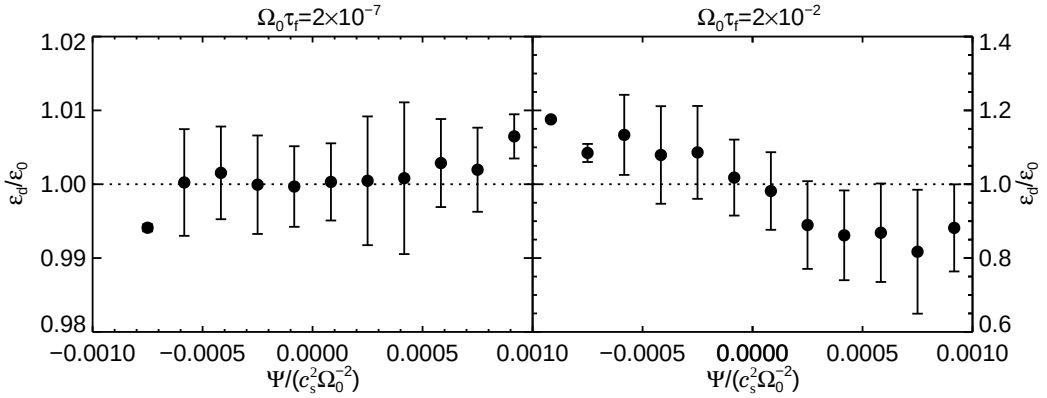

Fig. 18. Plot of dust-to-gas ratio in bins of the local vortex parameter $\Psi \equiv [-(\mathbf{u}\cdot\nabla)\mathbf{u}]\cdot\mathbf{f}(\mathbf{u})$ for the turbulent flow. Anticyclonic vortices have a negative value of Ψ, whereas for cyclonic vortices Ψ is positive. For the intermediate friction time run (see right panel:1cm sized particles with $\Omega\tau_f \approx 10^{-2}$), there is a clear anticorrelation between vortex parameter and dust-to-gas ratio. This is an indication that dust is being trapped in anticyclonic vortices which are features of the turbulent accretion disk flow. Particles in the left panel are too small to get concentrated (size is 0.1 μm). Taken from Johansen & Klahr 2005.

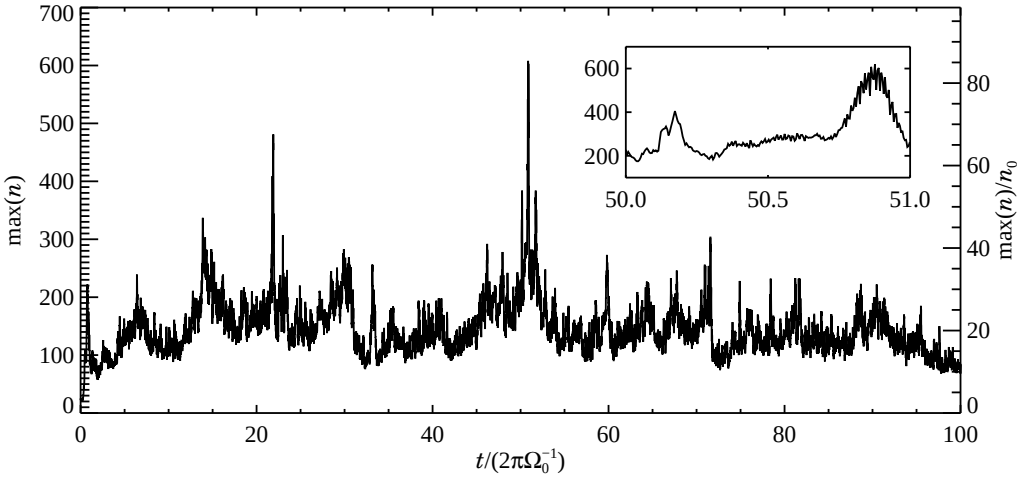

Fig. 19. The maximum number of particles in a single grid cell as a function of time for a run with meter-sized boulders, e.g. a Stokes number $\Omega\tau_f$ of about unity. The maximum density is generally around 20 times the average, but peaks at above 80 times the average particle density. The insert shows a magnification of the time between 50 and 51 orbits. Taken from Johansen, Klahr & Henning 2006.

and it is difficult to produce a population of boulders above this meter-size regime[3]. So the first defining property of planetesimals is that they move

[3] It is convenient to use the term meter-barrier, because for a distance of 5AU from the central object in a typical solar nebula the fastest drifting objects are of this dimension. Yet as the drift velocity depends on the gas density, temperature and local orbital period the fastest drifting objects will be smaller at greater distance

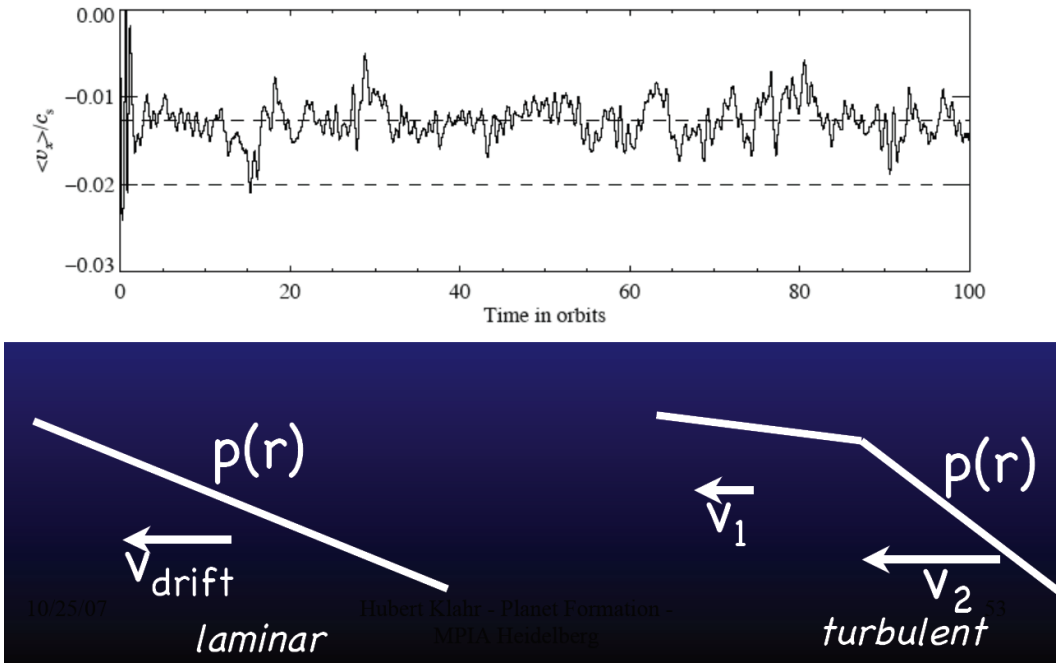

Fig. 20. The pressure fluctuations make the dust drift slower than in the laminar case. This can be understood as variations in the radial drift due to the variations in the radial pressure gradient. The average drift speed is smaller than the mean drift velocity as it is averaged over space and not time.

on Keplerian orbits and do not drift radially due to gas drag. The second property is that they can accrete and accumulate smaller objects by gravity, e.g. the gravitational pull at the surface of a planetesimal is stronger than the force exerted by the head wind. While we have a good understanding of how meter-sized objects grow from smaller dust grains via collisions and sticking, e.g. coagulation, and how planetesimals continue to form larger objects up to planetary cores, it is still a mystery how planetesimals form from meter-sized boulders. Boulders do not stick at collisions and even shatter at typical collision speeds. Finally they get lost into the central object by radial drift in a kind of rain-out event (Weidenschilling, 1980, 1984, 1995).

As gravity is the binding force for planetesimals it seems logical to invoke a formation scenario around a gravitational collapse of the dust phase in the solar nebula(Goldreich and Ward, 1973).

In the following sections we give an overview of recent numerical work the possibility of gravitational collapse of clouds formed by boulders (Johansen et al., 2006) and conclude with full 3D simulations of turbulence with particle feedback on the gas flow and self-gravitating boulders (Johansen et al., 2007).

from the star and larger in closer proximity to it.

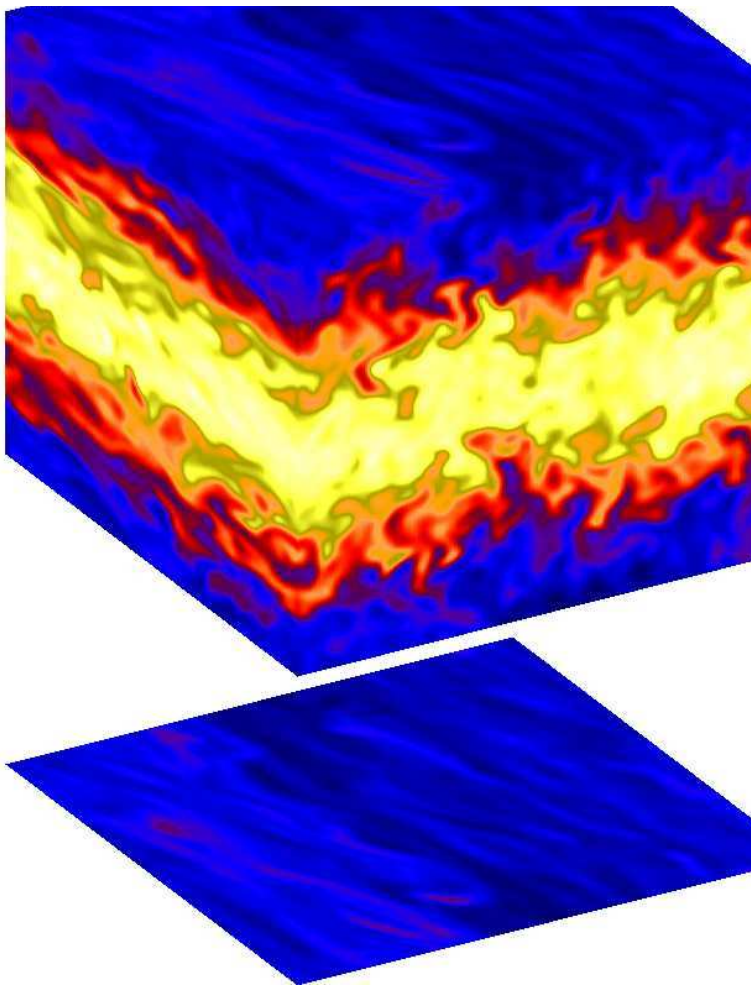

Fig. 21. Dust density contours at the sides of the simulation box for a short friction time run, i.e. $\Omega\tau_f = 2 \times 10^{-6}$, of sedimentation towards the midplane of the disk. The radial direction is towards the right while the shearing direction is towards left. The dust is concentrated around the mid-plane due to a vertical gravity field acting only on the dust, e.g. the gas does not feel the gravity and is thus not stratified. This setup is artificial but gives us the possibility to study the ideal case of unstratified turbulence before we introduce more realistic yet more complicated models. Turbulent transport alone prevents the further vertical settling of the dust layer. This configuration is statistically unchanged for at least one hundred orbits. Density fluctuations are an effect of the turbulence. Taken from Johansen & Klahr 2005.

6 Gravoturbulent Formation of Planetesimals

The previously mentioned investigations on particle concentrations in the short friction time regime (see Fig. 18) had to stop for technical reasons at centimeter-sized particles. Thus, the maximum density enhancements were only on the order of 20 %, yet strongly increasing with particle size. In a follow up study (Johansen et al., 2006) we focused on meter-sized objects, e.g.

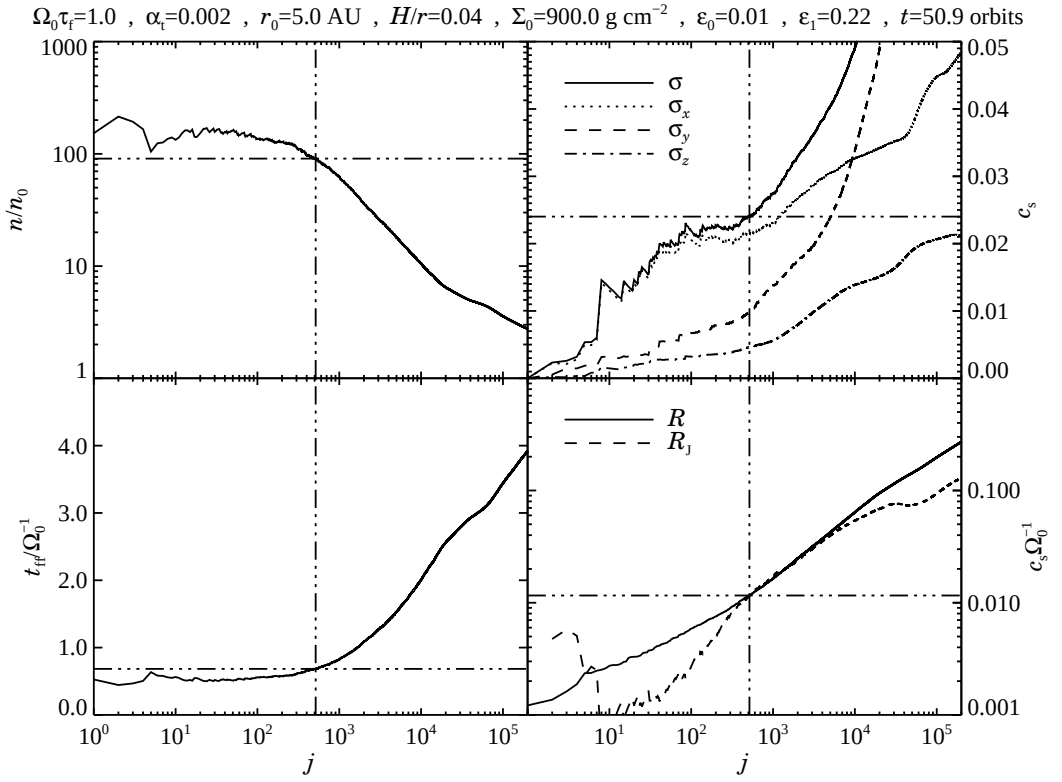

Fig. 22. Particle number density n in units of average density n_0, velocity dispersion σ in units of sound speed c_s, free-fall time t_{ff} relative to the clump life-time t_{cl}, and clump radius R together with Jeans radius R_J, all as a function of the number of included particles around the densest grid point in the box at a time of 50.9 orbits of the particular run. The vertical dot-dot-dot-dashed line separates the region of gravitational instability from the stable region as it gives the number of particles, at which the size of the clump is as big as a Jeans radius (see the lower right frame) for the choice of disc model parameters. Taken from Johansen, Klahr & Henning 2006.

boulders for which the friction time, respectively coupling time, is on the order of one orbital period. This means that we have a kind of resonance effect in the interaction between turbulence and particles, which leads to much higher dust to gas ratios (see 19), up to values of 80. These concentration live for a few orbital periods of the disk, before they decay again and are regenerated at some other location in the simulation. The densities turned out to be high enough that the gravitational attraction between them comes into play. Simple estimations of Jeans mass and collapse time indicate that bound objects are likely to form (see 22). In other words, the heaps of boulders do fit into the Roche-Lobe they generate, protecting them from the tidal torques by the star. At the same time the low yet sufficient braking by the gas drag decreases the kinetic energy in the cloud of boulders, i.e. leads to an efficient "cooling"(decreasing the rms velocity) and thus inevitably to a bound/solid object.

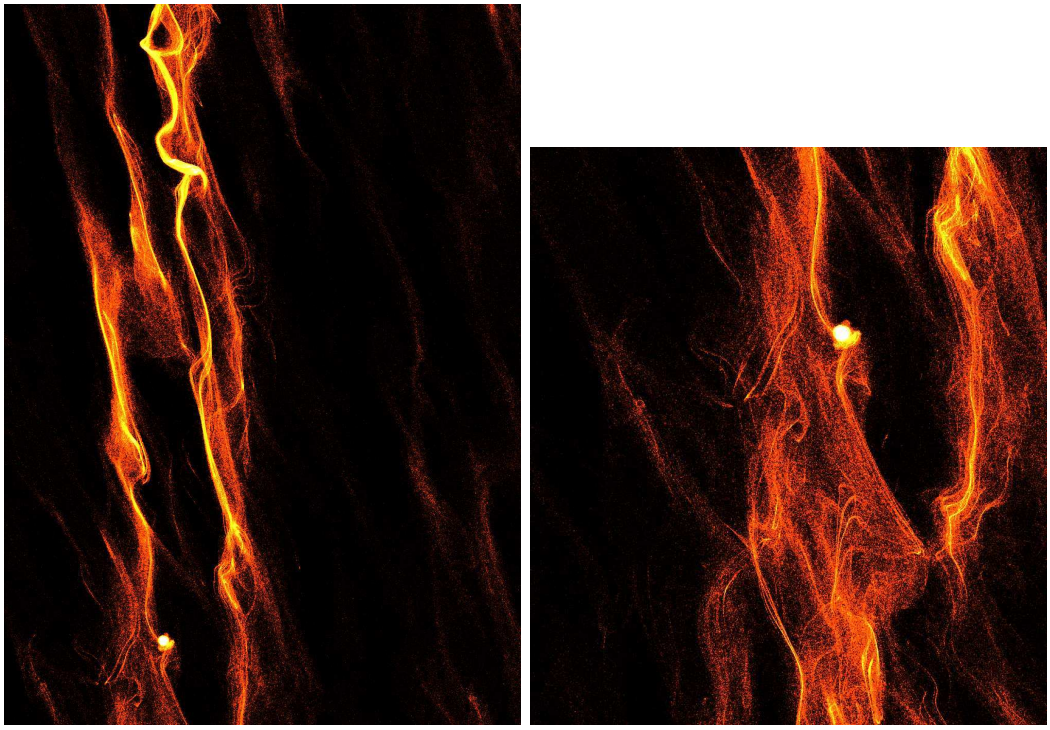

Fig. 23. The collapse of over-dense seeds into gravitationally bound boulder clusters: The two panels show the combined column density of the four different sizes of boulders at two different times. Over-dense bands initially contract radially, forming thin filaments with densities high enough for a full non-axisymmetric collapse into gravitationally bound clumps to take place. As time progresses, the Hill sphere increases in radius as the clusters grow in mass by accreting boulders from the turbulent flow (see *http://www.mpia.de/homes/johansen/research_en.php* for an animation of this simulation). The visualization was done with Partiview (*http://haydenplanetarium.org/universe/partiview/*).

7 The All in One Simulation

Inspired by the results from our previous work we developed our code further to incorporate particle feedback onto the gas, so the gas feels the friction with the particles, and gravitational attraction between the particles.

We also switched to a particle size distribution, where we postulate that conservatively 50% of dusty material is distributed in size between roughly 15 and 60 centimeters. The particle feedback had shown to lead to further enhancement of particle pileups via a streaming instability (Johansen and Youdin, 2007). These simulations found striking evidence for the formation of already minor planet-sized objects, e.g. about 1000 km in size (see 23 and 25) directly from the population of boulders. These results are discussed in detail in Johansen et al. (2007) to which we refer for further reading. The size of the formed objects decreases with resolution while the number of collapsing ob-

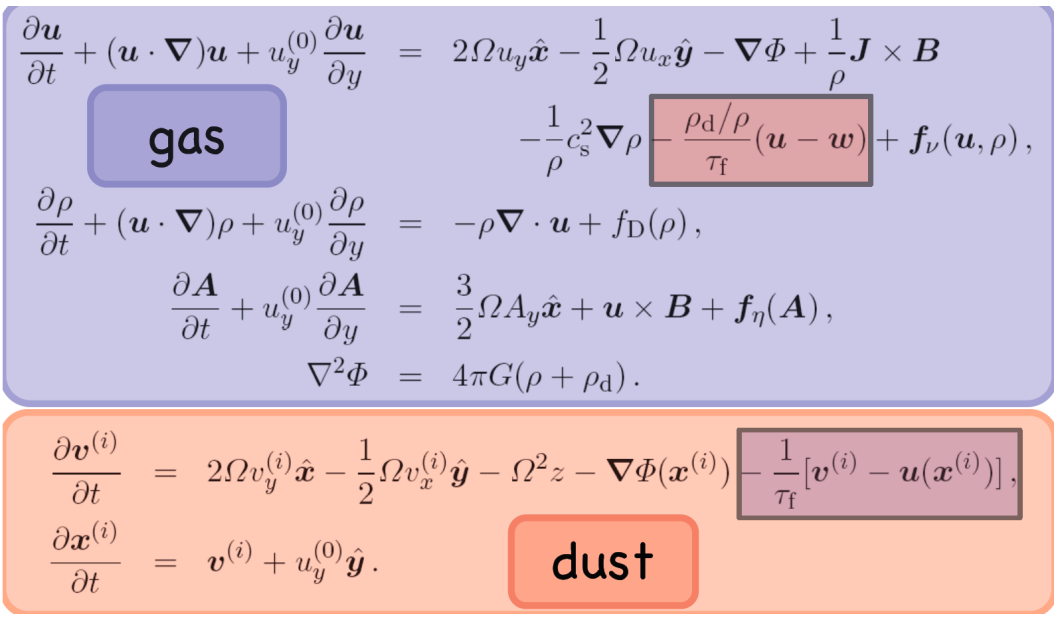

Fig. 24. The complete set of equations to be solved in the Pencil code for the all in one simulation. Note the two sets of equations for gas and particles as well as the coupling (friction) terms in the boxes.

jects increases (see 25). This is easy to understand because the resolved Jeans masses become smaller and smaller as the local densities increase. Convergence will be difficult to be achieved numerically, yet eventually the physical effects of rms speed of the boulder cloud will determine the smallest possible Jeans mass. Thus a final answer on the initial mass function for planetesimals must be postponed until refined adaptive mesh simulations or sophisticated sub-grid modeling become feasible. Interestingly our analytical considerations on the planetesimal size is in agreement with the estimations by Goldreich and Ward (1973). Nevertheless, we have to stress that the two models produce planetesimals of similar size, they do so through qualitatively different mechanisms (turbulent "trapping" versus pure gravitational instability).

The mechanism proposed here is quite promising to explain a rapid and efficient formation of planetesimals without increasing the dust content of a disk to many times the nominal value. Open questions remain in the determination of the initial mass function for planetesimals. This function will depend on the "cooling" properties of the gravitationally bound boulder clusters, e.g. the removal of dynamic pressure generated by the rms velocity of the boulders. The "cooling" behavior is early on provided by friction with the gas but will eventually be dominated by inelastic boulder-boulder collisions. A proper understanding of these collisions and especially collisional fragmentation will be vital for further progress with respect to planetesimal formation.

Collisional fragmentation is a general problem for meter-sized objects, not only in the collapse phase but even before that. So the next step in research must

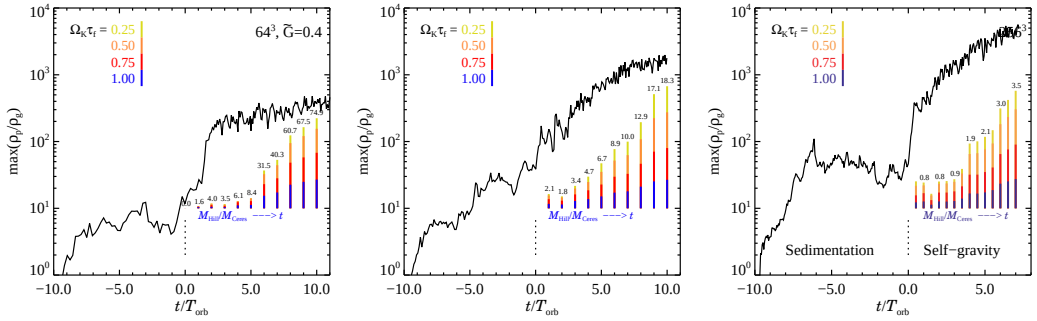

Fig. 25. Mass accretion onto a gravitationally bound cluster at three different numerical resolutions. The plots show the maximum bulk density of solids as a function of time, normalized by the average gas density. Drag force and vertical gravity are turned on at $t = -10$, while self-gravity and collisional cooling are turned on at $t = 0$. The density increases monotonically after the onset of self-gravity because gravitationally bound clusters of boulders form in the mid-plane. After only seven orbits peak densities in these clusters approach $10^4 \rho_g$ or a million times the average boulder density in the disc. The colored bars show the mass contained within the most massive Hill sphere in the box, in units of the mass of the 970 km radius dwarf planet Ceres ($M_{\rm Ceres} = 9.5 \times 10^{23}$ g). The most massive cluster in the highest resolution case accretes about $0.5 M_{\rm Ceres}$ per orbit (the entire box contains a total boulder mass of $50 M_{\rm Ceres}$). The cluster consists of approximately equal fractions of the three larger boulder sizes. The smallest size, with $\Omega_{\rm K}\tau_{\rm f} = 0.25$, is initially underrepresented with a fraction of only 15% because of the stronger aerodynamic coupling of those particles to the gas, but the fraction of small particles increases with time as the cluster grows massive enough to attract smaller particles as well. The mean free path inside the bound clusters is shorter than the size of the cluster, so any fragments formed in catastrophic collisions between the boulders will be swept up by the remaining boulders before being able to escape the cluster.

be an understanding of how dust grows to meter-sized boulders in a turbulent disk, using 3D-simulations that do not oversimplify the relevant physics. Only if we have the proper initial conditions of the boulder size distribution and in addition know the proper turbulent state of protoplanetary disks, will it be possible to put a solution to the planetesimal formation problem.

8 The core accretion - gas capture model

Once there is a sufficient population of planetesimals, e.g. the majority of dust was converted into more than kilometer sized objects, a period of oligarchic growth starts (Thommes et al., 2006). In this period the motion of the planetesimals is decoupled from the gas and strictly determined by the gravitational N-body interactions between the planetesimals. As a result of the gravitational interaction during close approaches the planetesimals increase their effective cross section for collisions (gravitational focusing: Safronov (1969)).

Collisions occur more frequently when the cross section, e.g. the particle size is larger. If particles attract each other during a close encounter, this attraction will increase the likelihood for a collision, which can be expressed as a larger cross section (with radius b) than given the actual particle size $r_{\min}$. Lets assume a two particles have the specific angular momentum $L = bv_0$ with respect to each other. At the closest approach the radial velocity component is zero. Then the angular momentum is

$$L = r_{\min} v_{\max}. \tag{14}$$

During the encounter energy is conserved

$$\frac{1}{4} m v_o^2 = \frac{1}{4} m v_{\max}^2 - \frac{G m^2}{r_{\min}}. \tag{15}$$

Angular momentum is also conserved

$$v_{\max} = \frac{b}{r_{\min}} v_o, \tag{16}$$

thus encounters with the impact parameter $b > r_{\min}$ will also lead to a collision, because the closest approach will be at $r_{\min}$.

$$b^2 = r_{\min}^2 + \frac{4 G m r_{\min}}{v_0^2} = r_{\min}^2 \left(1 + \frac{4Gm}{r_{\min} v_0^2} \right). \tag{17}$$

We see that the effective cross-section is effectively increased via gravitational focusing by the factor $F_g = 1 + \frac{4Gm}{r_{\min} v_0^2}$. One notices that this factor is the largest for massive particles and small relative velocities. This factor can also be written in terms of the ration of the escape velocity $v_e = \sqrt{\frac{4Gm}{r_{\min}}}$, e.g. $F_g = 1 + \left(\frac{v_e}{v_0}\right)^2$. The quantity $\theta = \left(\frac{v_e}{v_0}\right)^2 /2$ is known as the Safronov factor, a measure by how much the cross section is increased via gravity.

During the collisions larger and larger bodies form. The growth rates of planets can be estimated as follows: When we are letting two planetesimals collide with the sizes R_1 and R_2 then the cross section is is proportional to $R_s = R_1 + R_2$. The growth rate is proportional to the density of the planetesimal cloud ρ_p and the relative velocity v times the effective cross section:

$$\frac{\mathrm{d}m_p}{\mathrm{d}t} = \rho_p v \pi R_s^2 \left(1 + \left(\frac{v_e}{v_0} \right)^2 \right). \tag{18}$$

The density in planetesimals can be derived from the surface density of planetesimals Σ and the velocity dispersion v

$$\rho_p \approx \frac{\sqrt{3}}{2}\frac{\Sigma\Omega}{v}. \tag{19}$$

The $\sqrt{3}$ term results from the 3D nature of the velocity dispersion. Combining this with the equation for the growth rates we have:

$$\frac{\mathrm{d}m_p}{\mathrm{d}t} = \Sigma\Omega\pi R_s^2 F_g. \tag{20}$$

We learn from this equation that planets grow faster closer to the star, because Ω and Σ are larger there and that it is also easier beyond the snow line (see chapter by Alexander). Treating the growth rates more precisely one finds two distinct growth modes: 1.) All planetesimals are at a similar size and grow at the same speed. 2.) One object emerges from the population and eats up the rest (oligarchic growth) As a result not all objects grow equally in this process, but there are a few objects emerging from the planetesimal population (thus oligarchic growth) to become the future terrestrial planets and cores of the giant planets. This growth is the fastest closer to the star, as the densities and relative velocities are larger there than further away from the star. Eventually the planetary embryos are clearing out a gap around them in the planetesimal formation due to exchange of torques between the dominating body and the swarm of smaller guys. One can compare this to the shepherding moons in the rings of Saturn. Thus they have a critical mass (isolation mass) up to which they can grow, a mass which increases with the distance from the central object (see Fig. 26). This isolation mass can be estimated as follows. If the planet eats all the material in his feeding zone, e.g. the projection of the Hill sphere (with radius $R_h = \left(\frac{m_p}{3M_\star}\right)^{\frac{1}{3}}$) onto the planet's orbit (with radius r), then growth stops.

$$m_{isolation} \approx 4\pi r^2 \Sigma \left(\frac{m_p}{3M_\star}\right)^{\frac{1}{3}}. \tag{21}$$

Setting the planet mass m_p to the isolation mass yields

$$m_{isolation} \approx \frac{(4\pi r^2\Sigma)^{\frac{3}{2}}}{(3M_\star)^{\frac{1}{2}}}. \tag{22}$$

Plugging in numbers for the solar nebula leads to

$$m_{isolation} \approx 0.07 \left(\frac{a}{1\mathrm{AU}}\right)^3 \left(\frac{\Sigma}{10\mathrm{gcm}^{-2}}\right)^{3/2} M_\oplus. \tag{23}$$

At around Jupiters position conditions are conveniently optimal for its formation. Further out it takes longer than a typical life time of the disk of about 10 Million years and further in the isolation mass is too low to allow for gas accretion.

Here one can see that the terrestrial planets form faster than the cores of the giants, yet they stop at low masses, lower than observed today. The point is that there will be many planetary embryos to be formed in the inner part of the disk, which will then collide in the following hundreds of millions of years to form the final terrestrial planets. One of these collisions between proto-Earth and a Mars-size object lead most likely to the formation of our Moon from the collisional debris.

Jupiter and Saturn reached a critical mass of a few earth masses (see Fig. 27) while there was still gas around. Once the critical mass is reached there is slow accretion of gas, limited by the ability of the new planet to get rid of the accretion energy (both from gas and planetesimals) via radiation. Once the planet contains more gas than solids the cooling is more efficient and runaway accretion of gas occurs. This will only be stopped if their is no more gas in the vicinity of the planet, for instance by the gap clearing mechanism discussed later in this chapter. Although the physical processes are similar, the earlier discussion referred to gap-clearing in a planetesimal disk, while this discussion now refers to the qualitatively different process of gap-clearing in a (viscous) gaseous disc, and this distinction should be noted.

Neptune and Pluto on the other hand formed so slowly that there was almost no more gas to accrete at the time they had formed from the planetesimals. Thus their low content of gas.

This mechanism explains nicely why there are terrestrial planets close to star, followed by gas giants and lastly the gas-poor ice giants.

This picture was sufficient until the discovery of hot Jupiters in 1995. Those cannot be explained in this standard scenario. Either there was a very unusual centrally strongly concentrated planetesimal distribution, or the planet has formed further out and migrated inward, see below.

9 Planet disk interaction

It was speculated by some ingenious theoreticians that planets might migrate when they interact with a disk (Goldreich and Ward, 1980). Yet there was no need for migration to explain our own solar system. The situation changed after the discovery of the first exoplanets, which were gas giants and orbited

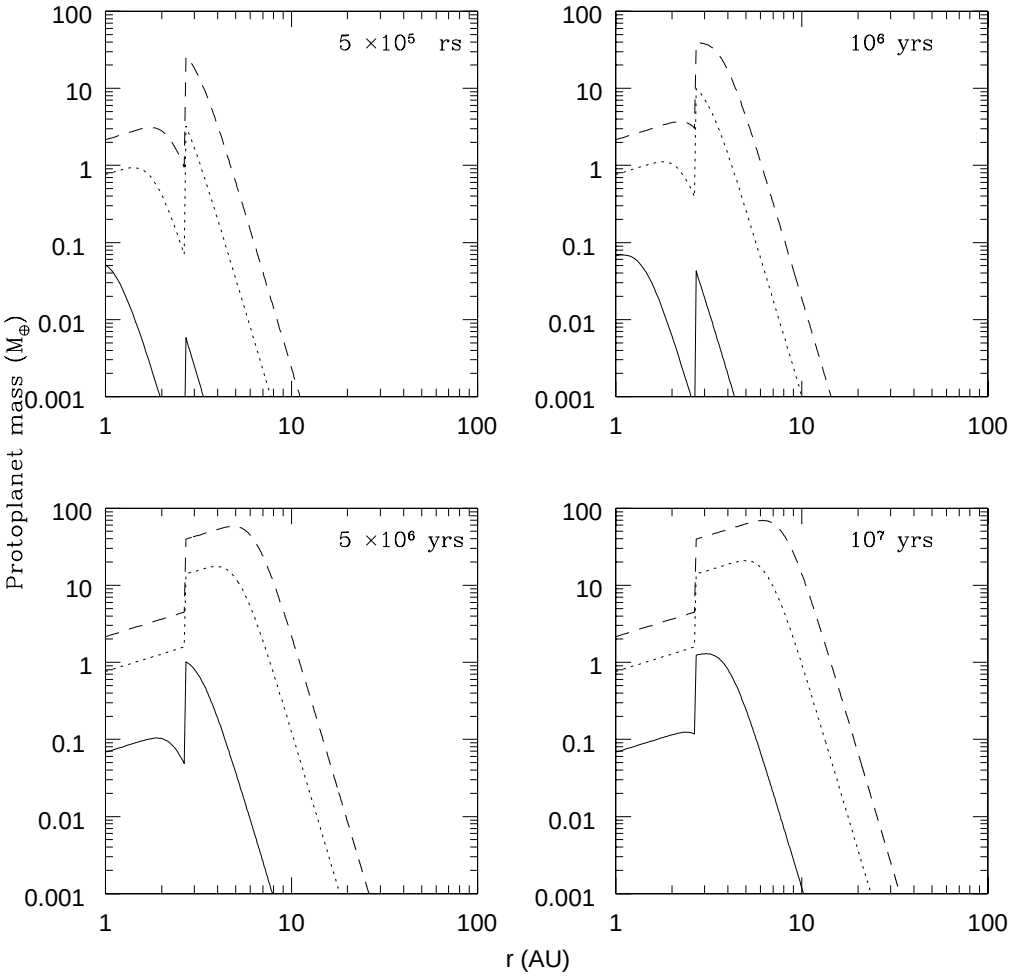

Fig. 26. The mass of the locally largest protoplanet as a function of stellocentric radius and time. The simple version of the oligarchic growth model, without the effect of planetesimal orbital decay by gas drag, is used to compute the curves; it gives a qualitatively correct picture of oligarchic growth but overestimates the final mass. The central star has a mass of $1M_{\odot}$, protoplanets and planetesimals have densities of 1.5 g cm^{-2}, planetesimals have a radius of 10 km, and an orbital spacing of $b = 10r_H$ between adjacent protoplanets is assumed. Gas and solids surface densities are scaled relative to the minimum-mass Solar nebula model. The calculation is performed for i) $1 \times \Sigma_{\rm gas}^{\rm min}$ and $1 \times \Sigma_{\rm solid}^{\rm min}$ (solid curve); ii) $5 \times \Sigma_{\rm gas}^{\rm min}$ and $5 \times \Sigma_{\rm solid}^{\rm min}$ (dotted curve); and iii) $10 \times \Sigma_{\rm gas}^{\rm min}$ and $10 \times \Sigma_{\rm solid}^{\rm min}$ (dashed curve). With kind permission by Ed Thommes.

their central object closer that does Mercury. Still it might be possible to explain such systems by in situ formation for extremely massive centrally condensed disks, nevertheless such configurations are generally regarded as unrealistic.

The alternative is that the planets formed further out and then migrated

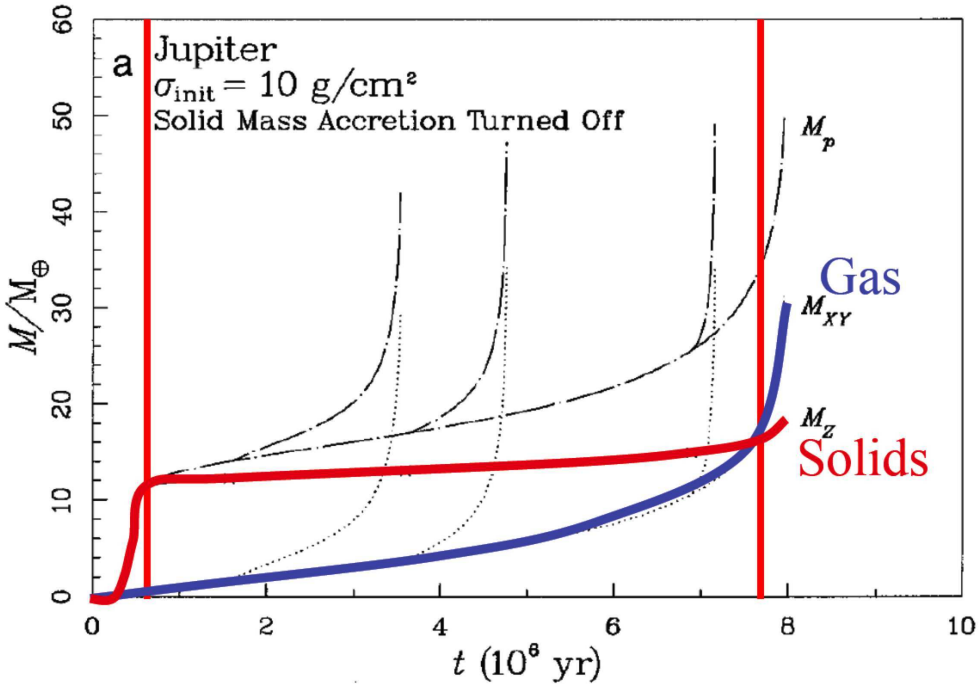

Fig. 27. Cumulative masses (gas and solids) as a function of time for the formation of Jupiter. The vertical lines separate the three growth phases: I: core accretion; II: gas and planetesimal accretion; III: gas runaway accretion. Reprinted with kind permission from Pollack et al. 1996.

inward. There are at least three different types of migration depending on what the mass of the planet is in comparison to the central object and to the disk mass. There is also the possibility that the migration is dominated by the interaction with the planetesimal disk rather than the gas disk. Finally planet-planet interaction will also influence the migration. This shows that the theory of planet migration was growing a lot over the last years, still there is no consistent unified theory yet. The problem is, that if the planets are migrating according to the standard models, then migration is too efficient in comparison to accretion of gas, thus the planets are likely to splash into the star before they become a gas giant. Also there is more than one theory to reason about stopping migration at close in radii. And the abundance of theories on the stopping mechanism (magnetic fields, disk truncation, resonances with another planets, etc.) shows that the situation is anything but understood. For a recent review on migration we refer to Papaloizou et al. (2007).

Here we want to give a simple description on the general mechanism of migration, which holds for all types of migration. Everything is dominated by tides. Lets refer to a system you might know: the moon is orbiting the earth. It deforms the earth from a sphere into an ellipsoid with one bulge pointing to the moon and the second one away from the moon. Yet this ideal situation would only be true if the earth would be rotating at the same rate as the

moon orbits the earth, e.g. always the same side of the earth faces the moon. As the earth is now rotating faster, e.g. one orbit per day and not per month, the bulges are propagating around the earth. We all know that from the tides twice per day at the beach. If the earth would have zero viscosity, the bulges would always be in phase with the moon, yet the earth interior is quite viscous and thus does not like to be deformed. For this reason the bulges are slightly advanced in the direction of the rotation of the earth and always a little before the moon. As a result the moon does see an asymmetric gravitational field, not a point source but a dipole field. The bulge facing the moon pulls on the moon stronger than the bulge on the far side, simply because the first one is closer. This first bulge pulls now not precisely orthogonal to the orbit of the moons, but a little bit along the orbit, transferring rotational energy from the earth onto the moon! As a result the earth rotates slower and slower. Originally the year had many more days than today for which there is fossil evidence. On the other hand the moon gains angular momentum and increases its distance towards the earth. Originally it was probably three times closer! Imagine what a sight that must have been in those days, with 10 times more light at full moon.

Planet disk interaction is now basically the same. The planet distorts the inner disk in a way (leading spirals) that it gains angular momentum and distorts the outer disk (trailing spirals) that it looses angular momentum (see the spirals in fig. 30). As the torques from the outer disk usually slightly dominate, planets are most of the time migrating inward.

To be more precise one can distinguish between three different modes of migration dependent on the mass of the planet and the surface density of the disk.

9.1 Type I migration

A planet imbedded in a disk exerts torques on the surrounding gas as it rotates around the star. This leads to certain resonances in the gas orbiting at radii further in as well as further out. These resonances are tidal waves, which are called Lindblad resonances. These resonances are now not rotational symmetric and thus can exert a torque on the planet themselves. The inner Lindblad resonances transfer angular momentum to the planet, where as the outer Lindblad resonances remove angular momentum from the planet. In general the outer Lindblad resonances prevail (Ward 1986) and the planet looses net angular momentum and migrates radially inward. The timescale of this type of migration depends on the planets mass. The migration rate can be as short as a few thousand years, which is, compared to the lifetime of the accretion disk and the growth time of planets, extremely short, rendering Type

I migration as quite an obstacle for planet formation. Future theories will have to explain a slowing down of this migration type via thermodynamical effects, magnetic fields, a dead zone etc. in order to leave time for the formation of the observed planets.

9.2 Type II migration

Larger planets start to open a gap around their orbit, which is in the order of the Hill spere in size. Now the perturbation onto the disk is so strong that one cannot treat the system by the linear Lindblad resonances any more. In this non-linear regime the planet migrates at the speed the accretion disk evolves, e.g. the planet migrates on the viscous time scale (see chapter by Lodato) in the order of 10^5 orbital periods. One can regard this as the disk pushing the planet along with the accretion flow while catching it in the center of the gap. When the outer wall gets closer, the planet migrates faster, when it moves to close to the inner wall of the gap it migrates slower, as it gains more angular momentum.

9.3 Type III migration

For intermediate planets in a mass rich disk a third mode could be possible, which is characterized by material in the horseshoe orbit region, see Fig. 28. The torque exerted by this material can be very strong as the material can get very close to the planet. If now predominantly mass flows from the inner disk via the gap to the outer disk, as it must if the planet is migrating inward, then this material has to use part of the horseshoe orbit behind the planet. This removes further angular momentum, increases the radial drift rate, which again lets more mass flow outward. This feedback leads to extremely fast migration. On the other hand if there is mass flow from the outer to the inner disk, then this flow occurs in front of the planet and angular momentum is transfered to the planet. This will lead here to outward migration with an increasing speed, because now also more material flows inward.

Most of the migration simulations were for artificially isothermal disks to keep the involved physics simple. In Klahr and Kley (2006) one can find a study on the evolution of an embedded protoplanet in a circumstellar disk using the 3D-radiation hydro code TraMP, and treat the thermodynamics of the gas properly in three dimensions (see Fig. 29). These simulations are now the basis to study the observability of planet-disk interaction (see Fig. 30) for upcoming instruments in the near as well as far-infrared.

Once we have such observations we will be able to test our theories on planet

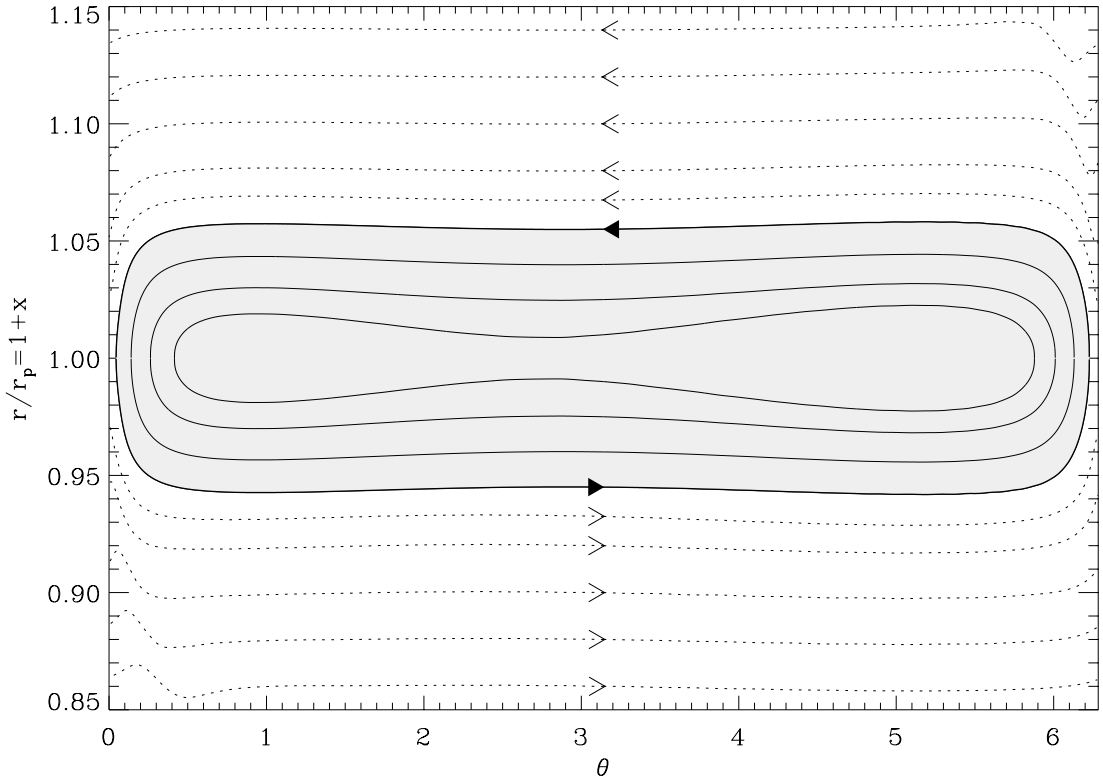

Fig. 28. Streamlines in the (φ, r) plane at an $m = 2$ corotation resonance. The grey shaded regions show the libration islands. One can notice that the outer and inner disk streamlines (in the white regions) are circulating, and exhibit radial oscillations with an amplitude that decreases with the distance to the corotation radius ($r = 1$). At the same time they do not show any winding, i.e. all these streamlines reach their maximum distance to the corotation radius at a constant azimuth $\varphi = 0,\ 2\pi/m, \ldots$ This behavior corresponds to the evanescent pressure supported waves in the corotation region, which have a purely imaginary radial wavevector (no winding and an exponential decay on the disk pressure scalelength). Reprinted with kind permission of Frederic Masset

formation. Until then we the theorists are urged to make testable predictions, such that we will not again be surprised by future detections such as now more than 10 years ago the Hot Jupiters. Predictions are also done as population synthesis models, which do now predictions for the Corot mission and the upcoming Kepler mission to detect planets down to a few earth radii (Alibert, 2005; Ida and Lin, 2005).

This manuscript is thought as a pedagogic text, thus it is not a review on the matter of planet formation. We therefore apologize that we do not mention many important contributors to the field and are pretty biased in our citations.

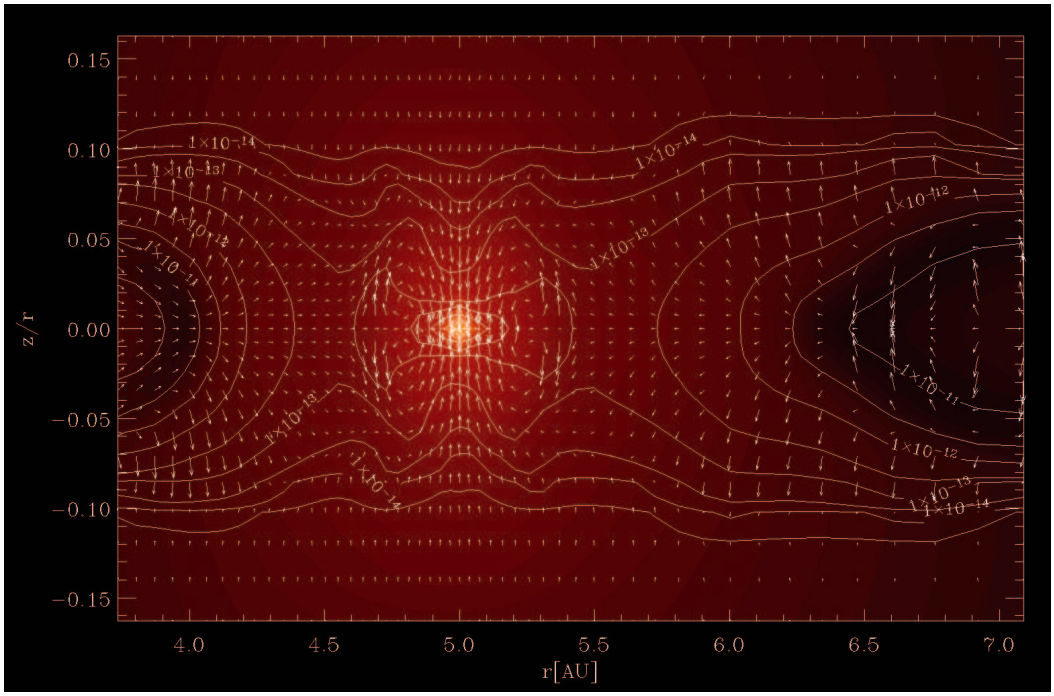

Fig. 29. Gap opening by planet: Temperature in the r - θ plane of the protoplanetary disk at the azimuthal location of the planet after 141 orbits. Brightness is logarithmic temperature (lighter = warmer) between 30 K and 1500 K, contours are equi-density lines (in g cm^3) and vectors give the logarithmic mass flux.

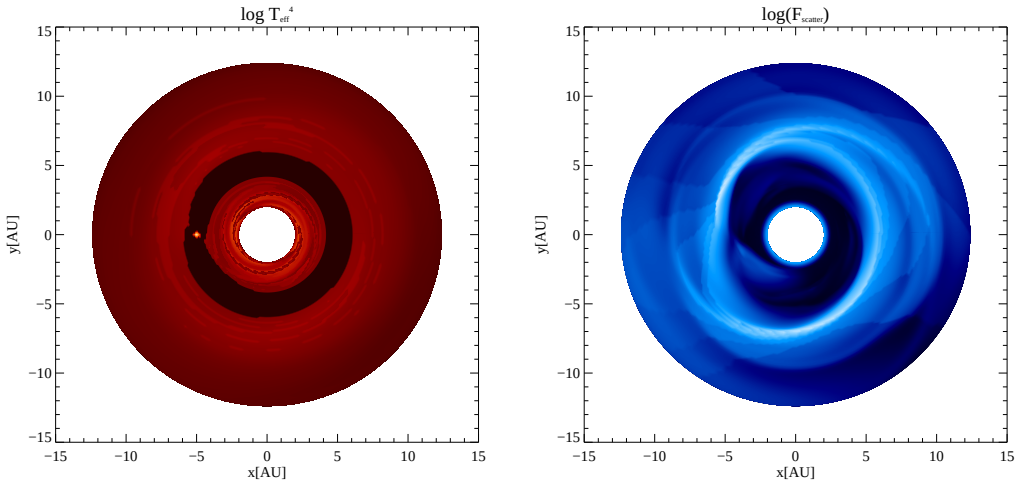

Fig. 30. Left: Emitted light. (e.g. ALMA)] and right: Scattered light (e.g. VLTI, LINC-NIRVANA, ELT). 3D radiation hydro simulation of planet-disk interaction for a study on the observability with various instruments. In the emitted light one can observe the gap and the hot blob of gas generated by the accretion onto the young planet. In the scattered light one will be able to observe the spiral waves generated by planetary torques.

References

Alibert Y Mordasini C and Benz W and Winisdoerffer C 2005 *Astronomy and Astrophysics* **434**, 343–353.

Bell K andCassen PM Klahr H Henning Th 1997 *ApJ*, **486**, 372–

Boss A P 1997 *Science* **276**, 1836–

Boss A P 2001 *ApJ* **563**, 367–

Boss A P 2004 *ApJ* **610**, 456–

Gammie C 2001 *ApJ* **553**, 174–

Balbus S A and Hawley J F 1998 *Reviews of Modern Physics* **70**, 1–53.

Balbus S A and Terquem C 2001 *ApJ* **552**, 235–247.

Barge P and Sommeria J 1995 *A&A* **295**, L1–L4.

Goldreich P and Tremaine S 1980 *ApJ* **241**, 425–441.

Goldreich P and Ward W R 1973 *ApJ* **183**, 1051–1062.

Hartmann L Calvet N Gullbring E and D'Alessio P 1998*ApJ* **495**, 385–400.

Hawley J F and Gammie C F and Balbus S A 1998*ApJ* **440**, 742–.

Ida S and Lin D N C 2005 *ApJ* **626**, 1045–1060.

Johansen A and Klahr H 2005 *ApJ* **634**, 1353–1371.

Johansen A, Klahr H and Henning T 2006 *ApJ* **636**, 1121–1134.

Johansen A, Klahr H and Mee T 2006 *MNRAS* **370**, L71-L75.

Johansen A, Oishi J, Mac Low M, Klahr H, Henning T and Youdin A 2007 *Nature* **448**(7157), 1022–1025.

Johansen A and Youdin A 2007 *ApJ* **662**, 627–641.

King A R and Pringle J E and Livio M 2007 *MNRAS* **376**, 1740–1746.

Klahr H and Bodenheimer P 2006 *ApJ* **639**, 432–440.

Klahr H and Kley K 2006 *Astronomy and Astrophysics* **445**, 747–758.

Klahr H and Brandner W **Planet formation - Theory, Observations, and Experiments** H. Klahr, W. Brandner (eds.), Cambridge (UK), Cambridge University Press, xvi + 302 pp., 2006, ISBN 0-521-86015-6

Lissauer J. J. 1993 *Annual Review of Astronomy and Astrophysics* **31**, 129–174.

Papaloizou J C B and Nelson R P and Kley W and Masset F S and Artymowicz P 2007 *Protostars and Planets V* 655–668.

Pollack J. B. Hubickyj O Bodenheimer P Lissauer J. J. Podolak M and Greenzweig Y 1996 *Icarus* **124**, 62–85.

Rafikov R 2005 *ApJ* **621**, 69–

Rafikov R 2007 *ApJ* **662**, 642–

Safronov V. S. 1969 *Evoliutsiia Doplanetnogo Oblaka i Obrazovanie Zemli i Planet (Moscow: Nauka) (English transl. Evolution of the Protoplanetary Cloud and Formation of Earth and the Planets [NASA Tech. Transl. F-677] [Jerusalem: Israel Program Sci. Transl.] [1972])*

Thommes E. W. Duncan M. J. Levison H. F. 2003 *Icarus* **161**, 431–455.

Ward W R 1980 *Icarus* **67**, 164–80.

Weidenschilling S J 1980 *Icarus* **44**, 172–189.

Weidenschilling S J 1984 *Icarus* **60**, 553–567.

Weidenschilling S J 1995 *Icarus* **116**, 433–435.